Mathematical Biology

Novel spatial profiles of some diffusive SIS epidemic models

Rui Peng[1] · Zhi-An Wang[2] · Guanghui Zhang[3] · Maolin Zhou[4]

Abstract

In this paper, we are concerned with two SIS epidemic reaction–diffusion models with mass action infection mechanism of the form SI, and study the spatial profile of population distribution as the movement rate of the infected individuals is restricted to be small. For the model with a constant total population number, our results show that the susceptible population always converges to a positive constant which is indeed the minimum of the associated risk function, and the infected population either concentrates at the isolated highest-risk points or aggregates only on the highest-risk intervals once the highest-risk locations contain at least one interval. In sharp contrast, for the model with a varying total population number which is caused by the recruitment of the susceptible individuals and death of the infected individuals, our results reveal that the susceptible population converges to a positive function which is non-constant unless the associated risk function is constant, and the infected population may concentrate only at some isolated highest-risk points, or aggregate at least in a neighborhood of the highest-risk locations or occupy the whole habitat, depending on the behavior of the associated risk function and even its smoothness at the highest-risk locations. Numerical simulations are performed to support and complement our theoretical findings.

✉ Zhi-An Wang
   mawza@polyu.edu.hk

   Rui Peng
   pengrui_seu@163.com

   Guanghui Zhang
   guanghuizhang@hust.edu.cn

   Maolin Zhou
   zhouml123@nankai.edu.cn

[1] School of Mathematical Sciences, Zhejiang Normal University, Jinhua 321004, Zhejiang, China

[2] Department of Applied Mathematics, The Hong Kong Polytechnic University, Hung Hom, Kowloon, Hong Kong

[3] School of Mathematics and Statistics, Huazhong University of Science and Technology, Wuhan 430074, China

[4] Chern Institute of Mathematics and LPMC, Nankai University, Tianjin 300071, China

 Springer

1 Introduction and existing results

The outbreak of the novel coronavirus disease 2019 (COVID-19) has caused tremendous impacts on public health and the global economy. As it is commonly recognized, population movement is a significant factor in the spread of many reported infectious diseases including COVID-19 (Balcan 2009; Brockmann and Helbing 2013; Jia 2020), and the lockdown and quarantine has turned out to be one of the most effective measures to reduce or even eliminate the infection (Kraemer 2020; Tian 2020). On the other hand, the importance of the population heterogeneity has also been observed in the complicated dynamical behaviour of the transmission of COVID-19 (Britton et al. 2020a, b; Di Lauro et al. 2021).

To gain a deeper understanding of the impact of population movement and heterogeneity on the transmission of epidemic diseases from a mathematically theoretical viewpoint, in the present work we are concerned with two SIS reaction–diffusion systems with mass action infection mechanism in a heterogeneous environment. We aim to study the spatial profile of population distribution as the movement rate of the infected individuals is controlled to be sufficiently small. Such kind of information may be useful for decision-makers to predict the pattern of disease occurrence and henceforth to develop more effective strategies of disease eradication. The mass action infection mechanism was first proposed in the seminal work of Kermack and McKendrick (1927), in which the disease transmission was assumed to be governed by a bilinear incidence function SI [one may also refer to Kermack and McKendrick (1991a, b, c) or Peng and Wu (2021)]. The systems under consideration in this paper are possibly the simplest yet basic SIS epidemic models.

The first model we will deal with in this work is the following coupled reaction–diffusion equations in one-dimensional space:

$$\begin{cases} S_t - d_S S_{xx} = -\beta(x)SI + \gamma(x)I, & 0 < x < L, \ t > 0, \\ I_t - d_I I_{xx} = \beta(x)SI - \gamma(x)I, & 0 < x < L, \ t > 0, \\ S_x = I_x = 0, & x = 0, L, \ t > 0, \\ S(x,0) = S_0(x) \geq 0, \ I(x,0) = I_0(x) \geq, \not\equiv 0, & 0 < x < L. \end{cases} \quad (1.1)$$

Here, $S(x,t)$ and $I(x,t)$ are respectively the population density of the susceptible and infected individuals at position $x \in [0, L]$ and time t; the homogeneous Neumann boundary condition means that no population flux crosses the boundary $x = 0, L$; d_S and d_I are positive constants measuring the motility of susceptible and infected individuals, respectively; and the functions β and γ are Hölder continuous positive functions in $[0, L]$ representing the disease transmission rate and the disease recovery rate, respectively.

Integrating the sum of the equations of (1.1), combined with the homogeneous Neumann boundary value conditions, we observe that

$$\int_0^L (S(x, t) + I(x, t))\, \mathrm{d}x = \int_0^L (S_0(x) + I_0(x))\, \mathrm{d}x =: N, \quad \forall t \geq 0.$$

Thus, the total population number in (1.1) is conserved all the time.

The system (1.1) was investigated in the recent works (Deng and Wu 2016; Wu and Zou 2016; Wen et al. 2018); in particular, when the movement of either the susceptible or infected population is restricted to be slow, the authors explored the profile of the spatial distribution of the disease modelled by (1.1). The understanding of such a profile amounts to determine the behavior of the so-called endemic equilibrium with respect to the small diffusion rate d_S or d_I. The endemic equilibrium of (1.1) is a positive steady state solution, which satisfies the following elliptic system:

$$\begin{cases} -d_S S_{xx} = -\beta(x)SI + \gamma(x)I, & 0 < x < L, \\ -d_I I_{xx} = \beta(x)SI - \gamma(x)I, & 0 < x < L, \\ S_x = I_x = 0, & x = 0, L, \\ \int_0^L (S(x) + I(x))\, \mathrm{d}x = N. \end{cases} \tag{1.2}$$

According to Deng and Wu (2016); Wu and Zou (2016); Wen et al. (2018), if $\min_{x \in [0,L]} \frac{\gamma(x)}{\beta(x)} < \frac{N}{L}$, for any small $d_I > 0$, (1.2) admits at least one positive solution (S, I), which is called an endemic equilibrium (EE for abbreviation) in terms of epidemiology; moreover, (S, I) satisfies $S, I \in C^2([0, L])$ and $S, I > 0$ on $[0, L]$.

As remarked in Wu and Zou (2016), it is a challenging problem to study the spatial profile of EE of (1.2) with respect to the small movement rate d_I of the infected population; in Wen et al. (2018), the authors provided a first result in this research direction. Indeed, they proved the following conclusion.

Theorem 1.1 (Wen et al. 2018, Theorem B) *Assume that* $\min_{x \in [0,L]} \frac{\gamma(x)}{\beta(x)} < \frac{N}{L}$. *Then as* $d_I \to 0$, *the EE* (S, I) *of* (1.2) *satisfies (up to a sequence of* d_I*) that* $S \to \hat{S}$ *uniformly on* $[0, L]$, *where* $\hat{S} \in C([0, L])$ *with* $\min_{[0,L]} \frac{\gamma(x)}{\beta(x)} \leq \hat{S}(x) \leq \max_{[0,L]} \frac{\gamma(x)}{\beta(x)}$, *and* $I \to \mu$ *weakly for some Radon measure* μ *with nonempty support in the sense of*

$$\int_0^L I(x)\zeta(x)\mathrm{d}x \longrightarrow \int_{[0,L]} \zeta(x)\mu(\mathrm{d}x), \quad \forall \zeta \in C([0, L]). \tag{1.3}$$

Obviously, Theorem 1.1 does not give a precise description for $\hat{S}$ and μ and hence the spatial profile of the susceptible and infected populations remains obscure. From the aspect of disease control, it becomes imperative to know an informative behavior of μ. In this paper, we manage to give a satisfactory result on the profile of $\hat{S}$ and μ.

In (1.1), some important factors such as the death and recruitment rates of population are ignored so that the total population number is a constant. In order to take into

account the death and recruitment rates of population, the following reaction–diffusion epidemic system was proposed in Li et al. (2018):

$$\begin{cases} S_t - d_S S_{xx} = \Lambda(x) - S - \beta(x)SI + \gamma(x)I, & 0 < x < L, \, t > 0, \\ I_t - d_I I_{xx} = \beta(x)SI - \big[\gamma(x) + \eta(x)\big]I, & 0 < x < L, \, t > 0, \\ S_x = I_x = 0, & x = 0, L, \, t > 0, \\ S(x, 0) = S_0(x) \geq 0, \, I(x, 0) = I_0(x) \geq, \not\equiv 0, \, 0 < x < L. \end{cases} \quad (1.4)$$

The recruitment term of the susceptible population is represented by the function $\Lambda(x) - S$ so that the susceptible is subject to the linear growth/death (Anderson and May 1979; Hethcote 2000); $\eta(x)$ accounts for the death rate of the infected. Here, Λ, η are assumed to be positive Hölder continuous functions on $[0, L]$. All other parameters have the same interpretation as in (1.1).

It is easily seen that the following elliptic problem

$$- d_S S_{xx} = \Lambda(x) - S, \; 0 < x < L; \quad S_x(0) = S_x(L) = 0 \quad (1.5)$$

admits a unique positive solution $\tilde{S}$. Then $(\tilde{S}, 0)$ is a unique disease-free equilibrium of (1.4). An EE of (1.4) satisfies the following ODE system:

$$\begin{cases} -d_S S_{xx} = \Lambda(x) - S - \beta(x)SI + \gamma(x)I, & 0 < x < L, \\ -d_I I_{xx} = \beta(x)SI - \big[\gamma(x) + \eta(x)\big]I, & 0 < x < L, \\ S_x = I_x = 0, & x = 0, L. \end{cases} \quad (1.6)$$

As one of the main results of Li et al. (2018), the following conclusion on the profile of EE of (1.6) with respect to small d_I was established.

Theorem 1.2 (Li et al. 2018, Theorem 3.2) *Assume that the set $\{x \in [0, L] : \beta(x)\tilde{S}(x) > \gamma(x) + \eta(x)\}$ is non-empty. As $d_I \to 0$, then any EE (S, I) of (1.6) satisfies (up to a subsequence of d_I) that $S \to \hat{S}$ uniformly on $[0, L]$, where $\hat{S} \in C([0, L])$ and $\hat{S} > 0$ on $[0, L]$, and $\int_0^L I \, dx \to \hat{I}$ for some positive constant $\hat{I}$.*

We would like to emphasize that the techniques used in the analysis of systems (1.2) and (1.6) are significantly different. In particular, for system (1.6), we encounter a free boundary problem of elliptic type, which requires new ideas and techniques to address. Additionally, it is not trivial to adapt the methods in this paper to a higher dimensional domain, and the extension of our results to a higher dimensional domain presents additional challenges due to the increased complexity of the problems.

The rest of paper is organized as follows. In Sect. 2, we state the main theoretical results, and in Sect. 3, we carry out the numerical simulations and discuss the implications of our results in terms of disease control. Section 4 is devoted to the proofs of the results presented in Sect. 2. In the appendix, we recall some known facts which will be used in the paper.

2 Statement of main results

In this section, we state the main findings of this paper on models (1.2) and (1.6). To proceed, we underline some terminologies frequently used throughout the paper. For model (1.2), we call $\frac{\gamma(x)}{\beta(x)}$ the *risk function*, and call each element of the set $\{x \in [0, L] : \frac{\gamma(x)}{\beta(x)} = \min_{x \in [0,L]} \frac{\gamma(x)}{\beta(x)}\}$ a *highest-risk point* (or *location*). Similarly, for model (1.6), we call $\frac{\gamma(x)+\eta(x)}{\beta(x)}$ the *risk function*, and call each element of the set $\{x \in [0, L] : \frac{\gamma(x)+\eta(x)}{\beta(x)} = \min_{x \in [0,L]} \frac{\gamma(x)+\eta(x)}{\beta(x)}\}$ a *highest-risk point* (or *location*).

2.1 Results for model (1.2)

For the sake of convenience, we set

$$k(x) = \frac{\gamma(x)}{\beta(x)}, \quad k_{min} = \min_{x \in [0,L]} k(x),$$

and

$$\Theta_k = \{x \in [0, L] : k(x) = k_{min}\}.$$

We note that when the risk function $k(x) = k$ is a positive constant, it follows from Wen et al. (2018) that $S(x) \equiv k$ is a constant, and in turn by the equation of I, we immediately see that $I = \frac{N}{L} - k$ is also a positive constant provided that $k < \frac{N}{L}$. In what follows, we do not consider such a trivial case and assume that $k(x)$ is non-constant on $[0, L]$.

We now state our main result on the asymptotic behavior of any EE (S, I) of (1.2) as $d_I \to 0$ as follows.

Theorem 2.1 *Assume that $k(x)$ is non-constant and $k_{min} < \frac{N}{L}$. Then as $d_I \to 0$, the EE (S, I) of* (1.2) *satisfies*

$$S(x) \to k_{min} \quad \text{uniformly for } x \in [0, L]. \tag{2.1}$$

The following assertions hold for the asymptotic behavior of I.

(i) If $\Theta_k = \{x_0\}$, then we have

$$I(x) \to (N - Lk_{min})\delta(x_0) \quad \text{weakly in the sense of (1.3)},$$

where $\delta(x_0)$ is the Dirac measure centered at x_0. Moreover, $I(x) \to 0$ locally uniformly in $[0, L] \setminus \{x_0\}$.

(ii) If $\Theta_k = [\varrho_1, \varrho_2]$ for some $0 < \varrho_1 < \varrho_2 < L$, then we have

$$I(x) \to 0 \quad \text{uniformly on } [0, \varrho_1] \cup [\varrho_2, L],$$

and

$$I(x) \to \hat{I}(x) \quad \textit{uniformly for } x \in [\varrho_1, \varrho_2],$$

where $\hat{I} \in C^2([\varrho_1, \varrho_2])$, $\hat{I} > 0$ in (ϱ_1, ϱ_2), and $\hat{I}$ is the unique positive solution of

$$\begin{cases} -\hat{I}_{xx} = \frac{\beta(x)}{d_S}(\hat{a} - \hat{I})\hat{I}, & \varrho_1 < x < \varrho_2, \\ \hat{I} = 0, & x = \varrho_1, \varrho_2, \\ \int_{\varrho_1}^{\varrho_2} \hat{I} \, dx = N - Lk_{min}, \end{cases} \tag{2.2}$$

where the positive constant $\hat{a}$ is uniquely determined by the integral constraint in (2.2).

Regarding Theorem 2.1, we would like to make some comments in order as follows.

Remark 2.1 In addition to the two cases treated in Theorem 2.1, we can handle some more general cases. In particular, we would like to make the following comments.

(i) If the set Θ_k contains only finitely many isolated points, say $\{x_i\}_{i=1}^{j}$ for some $j \geq 2$, then one can slightly modify the proof of Theorem 2.1(i) to show that $S \to k_{min}$ uniformly on $[0, L]$, and $I \to 0$ locally uniformly in $[0, L] \setminus (\{x_i\}_{i=1}^{j})$, and

$$I(x) \to \sum_{i=1}^{j} c_i \delta(x_i) \text{ weakly in the sense of (1.3)},$$

where $\delta(x_i)$ is the Dirac measure centered at x_i and the nonnegative constants c_i fulfill $\sum_{i=1}^{j} c_i = N - Lk_{min}$. Nevertheless, we can not determine the exact values of c_i; in other words, as $d_I \to 0$, it is unclear to us whether I concentrates at all x_i $(1 \leq i \leq j)$ or only some of them. The numerical results suggest that the former alternative holds; see Fig. 1 in Sect. 3.

(ii) If the set Θ_k contains at least one proper interval of $[0, L]$, by adapting the argument of Theorem 2.1(ii), we can show that $S \to k_{min}$ uniformly on $[0, L]$, and $I \to \hat{I}$ uniformly on $[0, L]$ with

$$\hat{I} = 0 \text{ on } [0, L] \setminus \Theta_k, \quad \int_{\Theta_k} \hat{I} \, dx = N - Lk_{min}.$$

In particular, if $\Theta_k = \left(\bigcup_{i=1}^{j_*} [\underline{\varrho}_i, \overline{\varrho}_i] \right) \bigcup \left(\bigcup \{x_i\}_{i=0}^{j^*} \right)$ for some $j_* \geq 1$, $j^* \geq 0$ with $[\underline{\varrho}_i, \overline{\varrho}_i] \cap [\underline{\varrho}_j, \overline{\varrho}_j] = \emptyset$ for $i \neq j$, then we can prove that

$$\hat{I} = 0 \text{ on } [0, L] \setminus \left(\bigcup_{i=1}^{j_*} (\underline{\varrho}_i, \overline{\varrho}_i) \right),$$

and in $(\underline{\varrho}_i, \overline{\varrho}_i)$ $(1 \leq i \leq j_*)$, either $\hat{I} = 0$ or $\hat{I} > 0$. Without loss of generality, assuming that $\hat{I}(x) > 0$ for $x \in \bigcup_{i=1}^{\hat{j}_*}(\underline{\varrho}_i, \overline{\varrho}_i)$ for some $1 \leq \hat{j}_* \leq j_*$, then in each such $(\underline{\varrho}_i, \overline{\varrho}_i)$, we can conclude that $\hat{I}$ solves

$$\begin{cases} -\hat{I}_{xx} = \frac{\beta(x)}{d_S}(\hat{a}_i - \hat{I})\hat{I}, & \underline{\varrho}_i < x < \overline{\varrho}_i, \\ \hat{I} = 0, & x = \underline{\varrho}_i, \overline{\varrho}_i, \end{cases}$$

where the positive constants $\hat{a}_i$ fulfill implicitly that

$$\sum_{i=1}^{\hat{j}_*} \int_{\underline{\varrho}_i}^{\overline{\varrho}_i} \hat{I} \, dx = N - Lk_{min}.$$

However, it seems rather challenging to prove whether $\hat{I}$ is positive on all intervals $(\underline{\varrho}_i, \overline{\varrho}_i)$ $(1 \leq i \leq j_*)$ or only on some of them. Our numerical results suggest that the former alternative holds; see Fig. 2 in Sect. 3.

(iii) The assertion in (ii) above suggests that if the highest-risk locations contain at least one interval, then the disease can not stay on any possible isolated highest-risk points once the infected individuals move slowly.

Remark 2.2 In the case (ii) of Theorem 2.1, if $\varrho_1 = 0$ (or $\varrho_2 = L$), the results of Theorem 2.1 still hold true if we replace the Dirichlet boundary condition of $\hat{I}$ in (2.2) at $\varrho_1 = 0$ (or $\varrho_2 = L$) by the Neumann boundary condition $\hat{I}_x(0) = 0$ (or $\hat{I}_x(L) = 0$). A similar remark applies to the case discussed in Remark 2.1(ii) above.

Remark 2.3 After this paper was finished, we noticed the work (Castellano and Salako 2022) in which the authors derived (2.1) and the convergence of the I-component in the case (i) of Theorem 2.1 in any spatial dimension in a more general setting; see Theorem 2.5(i) there. However, their result does not establish the convergence of the I-component within Θ_k in the case (ii) of Theorem 2.1 nor in the more general case mentioned by Remark 2.1; on the other hand, our proof of (2.1) and the convergence of the I-component outside of Θ_k is different from that of Castellano and Salako (2022).

2.2 Results for model (1.6)

We now turn to system (1.6). For the sake of simplicity, we assume that Λ in (1.6) is a positive constant, and also denote

$$h(x) = \frac{\gamma(x) + \eta(x)}{\beta(x)}, \quad h_{min} = \min_{x \in [0,L]} h(x),$$

and

$$\Theta_h = \{x \in [0, L] : h(x) = h_{min}\}.$$

Clearly, $\tilde{S}(x) = \Lambda$. We also enhance the existence condition of EE of (1.6) in Theorem 1.2 by imposing the following condition:

$$\Lambda > h(x) \quad \text{for all } x \in [0, L]. \tag{2.3}$$

We underline that the assumption that Λ is a positive constant and the condition (2.9) are of importance for our analysis. However, we speculate that the limiting profiles of the susceptible and infected populations may be similar in the more general scenario where Λ is a positive function and the set $\{x \in [0, L] : \beta(x)\tilde{S}(x) > \gamma(x) + \eta(x)\}$ is non-empty (note that the latter condition is necessary to guarantee the existence of an endemic equilibrium for all small $d_I > 0$).

Now we can state our main findings on the asymptotic behavior of any EE (S, I) of (1.6) as $d_I \to 0$. The first result reads as follows.

Theorem 2.2 *Assume that* (2.3) *holds. As $d_I \to 0$, then any EE (S, I) of (1.6) satisfies (up to a subsequence of d_I) that $S \to \hat{S}$ uniformly on $[0, L]$, and $I \to \mu$ weakly in the sense of* (1.3), *where μ is some Radon measure and $\hat{S}$ solves weakly in $W^{1,2}(0, L)$ the free boundary problem:*

$$- d_S \hat{S}_{xx} = \Lambda - \hat{S} - \eta(x)\mu(\{x\})\big|_{\{x \in [0, L]: \ \hat{S}(x) = h(x)\}}, \quad x \in (0, L). \tag{2.4}$$

Here, $\mu(\{x\})\big|_{\{x \in [0, L]: \ \hat{S}(x) = h(x)\}}$ is the restriction of μ on the set $\{x \in [0, L] : \hat{S}(x) = h(x)\}$; otherwise, $\mu(\{x\}) = 0$. Moreover we have the following properties for μ and $\hat{S}$.

(i) The Radon measure μ satisfies

$$\mu(\{x \in [0, L] : \ \hat{S}(x) \neq h(x)\}) = 0, \quad \mu(\{x \in [0, L] : \ \hat{S}(x) = h(x)\}) > 0. \tag{2.5}$$

(ii) The function $\hat{S} \in C([0, L])$ satisfies

$$h_{min} \leq \hat{S}(x) \leq h(x), \quad \forall x \in [0, L], \tag{2.6}$$
$$\Theta_h \subset \{x \in [0, L] : \ \hat{S}(x) = h(x)\}; \tag{2.7}$$

If $x_1, x_2 \in \Theta_h$ with $x_1 < x_2$ and $(x_1, x_2) \cap \Theta_h = \emptyset$, then

$$h_{min} < \hat{S}(x), \quad \forall x \in (x_1, x_2). \tag{2.8}$$

Theorem 2.2 states that the distribution of the susceptible population is generally non-uniform in space, despite its presence throughout the entire habitat, and that the disease will not become extinct in the entire habitat. However, Theorem 2.2 does not offer in-depth insights into the spatial distribution of the disease. As a result, our subsequent analysis aims to explore the properties of $\hat{S}$ and μ using specific yet representative risk functions h. The outcome will provide a more accurate depiction of the disease's profile. Indeed, we can obtain the following result for (1.6).

Theorem 2.3 *Let $\hat{S}$ and μ be given as in Theorem 2.2. Assume that $h \in C^2([0, L])$ and (2.3) holds. The following assertions hold.*

(i) If $-d_S h_{xx} \leq \Lambda - h$ in $(0, L)$, $h_x(0) \geq 0$ and $h_x(L) \leq 0$, then we have

$$\hat{S}(x) = h(x), \quad \forall x \in [0, L], \tag{2.9}$$

$$\mu(\{x\}) = \frac{\Lambda - h(x) + d_S h_{xx}(x)}{\eta(x)}, \quad \textit{a.e. for } x \in (0, L). \tag{2.10}$$

(ii) If h_x is non-decreasing on $[0, L]$ and $\Theta_h = \{\tau_0\}$ for some $0 \leq \tau_0 \leq L$, then the following assertions hold.

(a) When $0 < \tau_0 < L$, we have

$$\hat{S}(x) = h(x), \quad \forall x \in [\tau_1, \tau_2], \tag{2.11}$$

and in $[0, \tau_1) \cup (\tau_2, L]$, $\hat{S} < h$ satisfies

$$\begin{cases} -d_S \hat{S}_{xx}(x) = \Lambda - \hat{S}, & x \in (0, \tau_1) \cup (\tau_2, L), \\ \hat{S}_x(0) = 0, \quad \hat{S}_x(L) = 0, \\ \hat{S}(\tau_1) = h(\tau_1), \quad \hat{S}(\tau_2) = h(\tau_2), \end{cases} \tag{2.12}$$

and μ satisfies

$$\mu(\{x\}) = \frac{\Lambda - h(x) + d_S h_{xx}(x)}{\eta(x)}, \quad \textit{a.e. for } x \in (\tau_1, \tau_2), \tag{2.13}$$

$$\mu(\{x\}) = 0, \quad \forall x \in [0, \tau_1) \cup (\tau_2, L], \tag{2.14}$$

where the numbers τ_1, τ_2 with $0 < \tau_1 < \tau_0 < \tau_2 < L$ are uniquely determined by

$$\frac{e^{2d_S^{-1/2}\tau_1} - 1}{e^{2d_S^{-1/2}\tau_1} + 1} = -\frac{d_S^{1/2} h_x(\tau_1)}{\Lambda - h(\tau_1)}, \quad \frac{e^{2d_S^{-1/2}(\tau_2 - L)} - 1}{e^{2d_S^{-1/2}(\tau_2 - L)} + 1} = -\frac{d_S^{1/2} h_x(\tau_2)}{\Lambda - h(\tau_2)}. \tag{2.15}$$

(b) When $\tau_0 = L$, then we have the following assertions.

(b-1) If $\frac{e^{2Ld_S^{-1/2}}-1}{e^{2Ld_S^{-1/2}}+1} > -\frac{d_S^{1/2}h_x(L)}{\Lambda-h(L)}$, then (2.11) and (2.13) hold with $[\tau_1, \tau_2]$ replaced by $[\tau_1, L]$, $\mu([0, \tau_1)) = 0$, and on $[0, \tau_1]$, $\hat{S}$ satisfies

$$\begin{cases} -d_S\hat{S}_{xx}(x) = \Lambda - \hat{S}, & x \in (0, \tau_1), \\ \hat{S}_x(0) = 0, & \hat{S}(\tau_1) = h(\tau_1), \end{cases} \tag{2.16}$$

where $0 < \tau_1 < L$ is uniquely determined by the first equation in (2.15).

(b-2) If $\frac{e^{2Ld_S^{-1/2}}-1}{e^{2Ld_S^{-1/2}}+1} \leq -\frac{d_S^{1/2}h_x(L)}{\Lambda-h(L)}$, then $\hat{S}$ is the unique positive solution of

$$\begin{cases} -d_S\hat{S}_{xx}(x) = \Lambda - \hat{S}, & x \in (0, L), \\ \hat{S}_x(0) = 0, & \hat{S}(L) = h(L), \end{cases} \tag{2.17}$$

and μ satisfies

$$\mu([0, L)) = 0, \quad \mu(\{L\}) = \frac{\Lambda L - \int_0^L \hat{S}(x)\mathrm{d}x}{\eta(L)}. \tag{2.18}$$

(c) When $\tau_0 = 0$, then we have the following assertions.

(c-1) If $\frac{e^{2Ld_S^{-1/2}}-1}{e^{2Ld_S^{-1/2}}+1} > \frac{d_S^{1/2}h_x(0)}{\Lambda-h(0)}$, then (2.11) and (2.13) hold with $[\tau_1, \tau_2]$ replaced by $[0, \tau_2]$, $\mu((\tau_2, L]) = 0$, and on $[\tau_2, L]$, $\hat{S}$ satisfies

$$\begin{cases} -d_S\hat{S}_{xx}(x) = \Lambda - \hat{S}, & x \in (\tau_2, L), \\ \hat{S}_x(L) = 0, & \hat{S}(\tau_2) = h(\tau_2), \end{cases} \tag{2.19}$$

where $0 < \tau_2 < L$ is uniquely determined by the second equation in (2.15).

(c-2) If $\frac{e^{2Ld_S^{-1/2}}-1}{e^{2Ld_S^{-1/2}}+1} \leq \frac{d_S^{1/2}h_x(0)}{\Lambda-h(0)}$, then $\hat{S}$ is the unique positive solution of

$$\begin{cases} -d_S\hat{S}_{xx}(x) = \Lambda - \hat{S}, & x \in (0, L), \\ \hat{S}_x(L) = 0, & \hat{S}(0) = h(0), \end{cases} \tag{2.20}$$

and μ satisfies

$$\mu((0, L]) = 0, \quad \mu(\{0\}) = \frac{\Lambda L - \int_0^L \hat{S}(x)\mathrm{d}x}{\eta(0)}. \tag{2.21}$$

(iii) If h_x is non-decreasing on $[0, \varrho_1] \cup [\varrho_2, L]$ and $\Theta_h = [\varrho_1, \varrho_2]$ for some $0 < \varrho_1 < \varrho_2 < L$, then all the assertions in (ii)-(a) above hold, where the numbers τ_1, τ_2 satisfying $0 < \tau_1 < \varrho_1 < \varrho_2 < \tau_2 < L$ are uniquely determined by (2.15).

For model (1.2), our result shows that the infected population concentrates or aggregates only at the highest-risk locations. In sharp contrast, for model (1.6), our result suggests that the disease will occupy a neighborhood of the interior highest-risk locations or even occupy the whole habitat $[0, L]$, or concentrates only at the boundary highest-risk location, depending on the risk function h. More detailed discussions on the implications of our theoretical results, along with numerical simulations, will be given in Sect. 3.

We would like to make some remarks on Theorem 2.3 as follows.

Remark 2.4 It is worth mentioning that all the statements in Theorem 2.3 except the expression (2.13) for the Radon measure μ remain true provided that the risk function $h \in C^1([0, L])$. Such a comment also applies to Lemmas 4.1-4.4 in Sect. 4.

Remark 2.5 (i) It is clear that Theorem 2.3(i) holds if $h < \Lambda$ is a constant or more generally h is a unique solution to the following problem:

$$\begin{cases} -d_S h_{xx} = \Lambda - h, & x \in (0, L), \\ h(0) = \sigma_1, \ h(L) = \sigma_2, \end{cases}$$

where $0 < \sigma_1, \sigma_2 < \Lambda$. When $h_x(0) > 0$, the change of the derivatives from $S_x(0) = 0$ to $\hat{S}_x(0) = h_x(0) > 0$ would suggest that I should experience the concentration phenomenon at $x = 0$ (that is, $I(0) \to \infty$) as $d_I \to 0$. The same remark applies to the case of $h_x(L) < 0$.

(ii) In contrast to Theorem 2.3(i), it is easily seen that $\hat{S} \not\equiv h$ on $[0, L]$ provided that $-d_S h_{xx}(x^*) > \Lambda - h(x^*)$ for some $x^* \in (0, L)$.

(iii) Clearly, the assertions of Theorem 2.3(ii)-(b1) hold if $h_x(L) = 0$ and the assertions of Theorem 2.3(ii)-(c1) hold if $h_x(0) = 0$.

(iv) In a general case that Θ_h contains an interior isolated point and h_x is non-decreasing in a neighbourhood of such a point, we can conclude that (2.9) and (2.10) hold in some neighbourhood of this point; if Θ_h contains an interval, a similar conclusion also holds. See Lemma 4.1 and Lemma 4.3 below.

3 Discussions and numerical simulations

In recent years, many reaction–diffusion models have been proposed to investigate the transmission dynamics of infectious diseases in a heterogeneous environment. For example, models associated with (1.1) have been studied in Allen et al. (2008); Du and Peng (2016); Deng and Wu (2016); Gao (2019); Li and Bie (2019); Li et al. (2017a, b, 2018); Magal et al. (2018, 2019); Peng (2009); Peng and Liu (2009); Peng and Yi (2013); Peng and Zhao (2012); Suo and Li (2019); Tong and Lei (2018); Wu and Zou (2016). When the random diffusion is not present, such kind of models have been explored in Allen et al. (2007, 2009); Gao and Dong (2020); Gao and Ruan (2011); Li and Shuai (2009); Li and Peng (2019); Vargas-De-Leon and Korobeinikov (2013); Wodarz et al. (2002); Wodarz and Nowak (2000) and the references therein. One may also refer to Cui and Lou (2016); Ge et al. (2015); Han and Lei (2019); Lei et al.

(2018); Li et al. (2018); Lei et al. (2020); Li et al. (2020); Song et al. (2019); Wang and Wu (2023); Wang and Wang (2021); Zhu and Wang (2020a, b) for relevant studies on the effect of random diffusion on the dynamics of infectious diseases.

In this paper, we have investigated the positive steady state solution (namely, EE) of the SIS epidemic reaction–diffusion models (1.2) and (1.6), in which the disease transmission is governed by the well-known mass action infection mechanism, due to Kermack and McKendrick (1927). In model (1.2), the total population number of the susceptible and infected populations is a constant, while in model (1.6), the total population number is varying, which results from the inclusion of the recruitment for the susceptible population and the death of the infected population. Our purpose is to determine the spatial profile of EE as the movement rate d_I of the infected individuals tends to zero. Such kind of information may be useful for decision-makers to predict the pattern of disease occurrence and henceforth to develop effective disease control strategies.

The previous works (Li et al. 2017b; Wen et al. 2018) derived partial results regarding the spatial profile of EE for (1.2) and (1.6) as $d_I \to 0$; however, a precise characterization for the distribution of susceptible and infected populations is lacking. In the present work, we have provided a comprehensive understanding on this issue. Below we shall summarize the main theoretical findings of this paper, which will also be supported or complemented by our numerical simulation results. We remark that our numerical computations are directly performed to the parabolic systems (1.1) and (1.4) by the MATLAB PDEPE solver. Then the time-independent profiles of (1.1) and (1.4) are used to approximate the solution profiles of corresponding steady-state systems (1.2) and (1.6), respectively. All solution profiles are plotted at time $t = 400$ without further mention below.

3.1 Profile of EE of model (1.2) as $d_I \to 0$

As pointed out before, when the risk function $k(x) = \frac{\gamma(x)}{\beta(x)}$ is a constant on the entire habitat $[0, L]$, then $(k, \frac{N}{L} - k)$ is the unique EE of (1.2) provided that $k < \frac{N}{L}$, while $(\frac{N}{L}, 0)$ is the unique disease-free equilibrium of (1.2) provided that $k \geq \frac{N}{L}$. Indeed, in such a trivial case, one can follow the same analysis as in Deng and Wu (2016, Theorem 4.1) to conclude that $(k, \frac{N}{L} - k)$ is a global attractor of (1.1) if $k < \frac{N}{L}$ and $(\frac{N}{L}, 0)$ is a global attractor of (1.4) if $k \geq \frac{N}{L}$. Thus, unless otherwise specified, we always assume below that the risk function $k(x) = \frac{\gamma(x)}{\beta(x)}$ is *non-constant* on $[0, L]$.

According to Theorem 2.1, for model (1.2), one finds that the susceptible population S converges to the positive constant k_{min} as $d_I \to 0$, which means that the susceptible will always distribute homogeneously on the entire habitat once the movement of the infected individuals is restricted to be sufficiently small. Nevertheless, the profile of the infected population I as $d_I \to 0$ crucially depends on the distribution behavior of the highest-risk set Θ_k of the risk function $k(x)$. More precisely, concerning the profile of I for model (1.2), we have the following findings.

(i) If Θ_k consists of a single point, then I must concentrate only at such a highest-risk point.
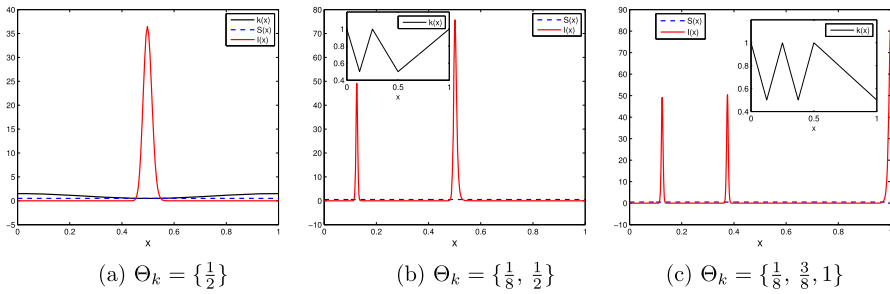
Fig. 1 Numerical simulations of the solution profile of model (1.2), where $L = 1$, $N = 2$, $d_S = 1$, $d_I = 10^{-7}$, $\beta(x) = 1 + \frac{1}{2}\sin(2\pi x)$, $\gamma(x) = k(x)\beta(x)$, $k_{\min} = \frac{1}{2}$ and $k(x)$ is chosen as follows. In (**a**), $k(x) = 1 + \frac{1}{2}\cos(2\pi x)$. In (**b**), $k(x) = 1 - 4x$, $0 \leq x < \frac{1}{8}$; $k(x) = 4x$, $\frac{1}{8} \leq x < \frac{1}{4}$; $k(x) = \frac{3}{2} - 2x$, $\frac{1}{4} \leq x < \frac{1}{2}$; $k(x) = x$, $\frac{1}{2} \leq x \leq 1$. In (**c**), $k(x) = 1 - 4x$, $0 \leq x < \frac{1}{8}$; $k(x) = 4x$, $\frac{1}{8} \leq x < \frac{1}{4}$; $k(x) = 2 - 4x$, $\frac{1}{4} \leq x < \frac{3}{8}$; $k(x) = 4x - 1$, $\frac{3}{8} \leq x < \frac{1}{2}$; $k(x) = \frac{3}{2} - x$, $\frac{1}{2} \leq x \leq 1$

(ii) If Θ_k contains only multiple isolated points, it follows from Remark 2.1 that I will also concentrate at least at one of those highest-risk points, and the disease will vanish elsewhere. As shown in Fig. 1a–c for three typical cases, our simulation results suggest that I should concentrate at all such highest-risk points, though the population number of I at each such highest-risk point may vary, depending on the functions β, γ.

(iii) If Θ_k contains at least one proper interval, then no concentration phenomenon occurs for the disease distribution, and the infected population will aggregate only on such intervals consisting of highest-risk points, regardless of whether there are isolated highest-risk points or not (see Fig. 2a, b). Indeed, our numerical results indicate that the infected population will aggregate on all such intervals consisting of highest-risk points (see Fig. 2c); however the population number of I at each such interval may be different, depending on the functions β, γ.

3.2 Profile of EE of model (1.6) as $d_I \to 0$

For model (1.6), for the general Hölder continuous risk function h, under the condition (2.3), as $d_I \to 0$, we know from Theorem 2.2 that the susceptible population S converges to a positive function $\hat{S}$, which is non-constant unless h is constant.

The infected population I converges to a positive Radon measure μ, whose support is contained in the region where $\hat{S}$ touches h, and if additionally the risk function h is of C^2, we see from Lemma 4.1 and Lemma 4.3 in Sect. 4 that the infected population aggregates at least in a neighborhood of the highest-risk locations.

Furthermore, when $h \in C^2([0, L])$, in light of Theorem 2.3, one can draw the following conclusions concerning the asymptotic profile of I.

(i) For any risk function h satisfying

$$-d_S h_{xx} \leq \Lambda - h \quad \text{in } (0, L), \quad h_x(0) \geq 0, \quad h_x(L) \leq 0,$$
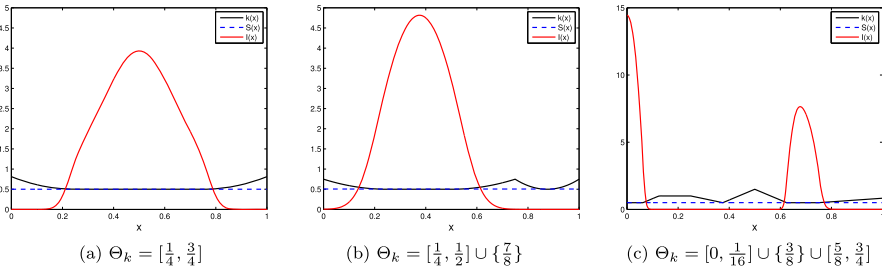
Fig. 2 Numerical simulations of the solution profile of model (1.2), where $L = 1$, $N = 2$, $d_S = 1$, $d_I = 10^{-5}$, $\beta(x) = 1$, $\gamma(x) = k(x)\beta(x)$, $k_{\min} = \frac{1}{2}$ and $k(x)$ is chosen as follows. In (a), $\Theta_k = [\frac{1}{4}, \frac{3}{4}]$, $k(x) = \frac{1}{2} + 5(x - \frac{1}{4})^2, 0 \le x < \frac{1}{4}$; $k(x) = \frac{1}{2}$, $\frac{1}{4} \le x < \frac{3}{4}$; $k(x) = \frac{1}{2} + 5(x - \frac{3}{4})^2$, $\frac{3}{4} \le x \le 1$. In (b), $\Theta_k = [\frac{1}{4}, \frac{1}{2}] \cup \{\frac{7}{8}\}$, $k(x) = \frac{1}{2} + 4(x - \frac{1}{4})^2$, $0 \le x < \frac{1}{4}$; $k(x) = \frac{1}{2}$, $\frac{1}{4} \le x < \frac{1}{2}$; $k(x) = \frac{1}{2} + 4(x - \frac{1}{2})^2$, $\frac{1}{2} \le x < \frac{3}{4}$; $k(x) = \frac{1}{2} + 16(x - \frac{7}{8})^2$, $\frac{3}{4} \le x \le 1$. In (c), $\Theta_k = [0, \frac{1}{16}] \cup \{\frac{3}{8}\} \cup [\frac{5}{8}, \frac{3}{4}]$, $k(x) = \frac{1}{2}$, $0 \le x < \frac{1}{16}$; $k(x) = 8x$, $\frac{1}{16} \le x < \frac{1}{8}$; $k(x) = 1$, $\frac{1}{8} \le x < \frac{1}{4}$; $k(x) = 2 - 4x$, $\frac{1}{4} \le x < \frac{3}{8}$; $k(x) = 8x - \frac{5}{2}$, $\frac{3}{8} \le x < \frac{1}{2}$; $k(x) = \frac{11}{2} - 8x$, $\frac{1}{2} \le x < \frac{5}{8}$; $k(x) = \frac{1}{2}$, $\frac{5}{8} \le x < \frac{3}{4}$; $k(x) = \frac{2}{3}x$, $\frac{3}{4} \le x \le 1$
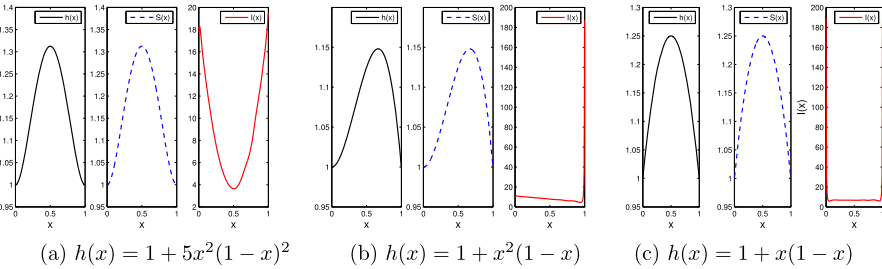

Fig. 3 Numerical simulations of the solution profile of model (1.6), where $\beta(x) = 1 + \frac{1}{2}\sin(2\pi x)$, $\eta(x) = 1$, $\gamma(x) = h(x)\beta(x) - \eta(x)$, $d_S = 1$, $d_I = 10^{-8}$, $\Lambda = 10$. In (a), $h(x) = 1 + 5x^2(1 - x)^2$, in (b), $h(x) = 1 + x^2(1 - x)$, and in (c), $h(x) = 1 + x(1 - x)$

and condition (2.3) (for instance, $h < \Lambda$ is a positive constant), the infected population must occupy the entire habitat, and it also forms the concentration phenomenon at the boundary point $x = 0$ (or $x = 1$) if $h_x(0) > 0$ (or $h_x(1) < 0$), which is also the highest-risk location; see Theorem 2.3(i) and the numerical illustrations in Fig. 3a–c.

(ii) For any convex risk function h (i.e., $h_{xx} \ge, \not\equiv 0$ on $[0, L]$) fulfilling (2.3), the infected population usually stays only in part of the habitat. In particular, by Theorem 2.3(ii)(iii), we can observe the following behaviors.

(ii-a) If the highest-risk set Θ_h contains only one point, denoted by τ_0, then the distribution behavior of the infected population is affected by whether τ_0 is a boundary point or an interior point. More precisely, when τ_0 is an interior point, then the infected population resides in a certain left neighborhood of τ_0, staying away from the boundary points $x = 0$ and $x = 1$. In fact, such a neighborhood can be calculated through the formula (2.15). One may further refer to Fig. 4a.

However, if τ_0 is a boundary point, say $\tau_0 = L$, then the infected population stays in a certain neighborhood of L provided

$$\frac{e^{2Ld_S^{-1/2}} - 1}{e^{2Ld_S^{-1/2}} + 1} > -\frac{d_S^{1/2}h_x(L)}{\Lambda - h(L)},$$

while the infected population concentrates only at L provided

$$\frac{e^{2Ld_S^{-1/2}} - 1}{e^{2Ld_S^{-1/2}} + 1} \leq -\frac{d_S^{1/2}h_x(L)}{\Lambda - h(L)}.$$

Since $h_x(L) \leq 0$ in this situation, the infected population stays in a certain neighborhood of L provided for all $d_S > 0$ if $h_x(L) = 0$. If $h_x(L) < 0$, it should be noted that the function

$$q(d_S) = d_S^{-1/2}\frac{e^{2Ld_S^{-1/2}} - 1}{e^{2Ld_S^{-1/2}} + 1} + \frac{h_x(L)}{\Lambda - h(L)}$$

deceases in $d_S \in (0, \infty)$, $\lim_{d_S \to 0} q(d_S) = \infty$ and $\lim_{d_S \to \infty} q(d_S) = \frac{h_x(L)}{\Lambda - h(L)} < 0$. As a result, there is a unique $d_S^* > 0$ such that $q(d_S^*) = 0$, and in turn the infected population stays in a left neighborhood of L for $0 < d_S < d_S^*$, and the infected population concentrates only at L for all $d_S \geq d_S^*$.

(ii-b) If the highest-risk set Θ_h contains only an interval, then the infected population resides in a certain neighborhood of such an interval. Again, such a neighborhood can be calculated through the formula (2.15). See the numerical simulation in Fig. 4b.

(ii-c) For a general Hölder continuous risk function h, we can conclude that the disease must exist in all isolated highest-risk point(s) and a neighborhood of each highest-risk interval if exists; nevertheless, it is challenging to give a precise characterization for the distribution behavior of the susceptible and infected populations, due to the mathematical difficulties on the analysis of the free boundary problem (2.4). We have performed the numerical simulations in Fig. 5a, b as an illustration.

In what follows, we would like to make some more discussions on (ii-a) above in the case that τ_0 is a boundary point. For example, we take $\tau_0 = L$, and also assume that $h_x(L) < 0$. On the one hand, by fixing $h_x(L)$, we have known from (ii-b) that large diffusion rate d_S can result in the disease concentration only at the location L and small diffusion rate d_S will cause the disease to distribute in a left neighborhood of L. On the other hand, once d_S is fixed, the concentration phenomenon happens only if $-h_x(L)$ is properly large. This motivates us to see whether a similar concentration phenomenon could occur at an interior isolated highest-risk point if the risk function h is merely Hölder continuous. To illustrate this phenomenon, let us consider the

(a) $\Theta_h = \{\frac{1}{2}\}$ (b) $\Theta_h = [\frac{1}{4}, \frac{3}{4}]$
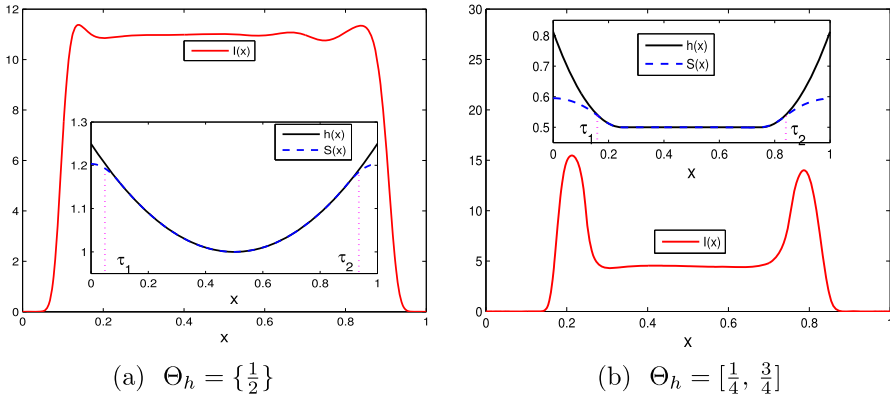
Fig. 4 Numerical simulations of the solution profile of model (1.6), where $\beta(x) = 1 + \frac{1}{2}\sin(2\pi x)$, $\eta(x) = 1$, $\gamma(x) = h(x)\beta(x) - \eta(x)$, $d_S = 1$, $d_I = 10^{-10}$, $\Lambda = 10$, and $h(x) = 1 + (x - \frac{1}{2})^2$ in (**a**), while in (**b**), $h(x) = \frac{1}{2} + 5(x - \frac{1}{4})^2$, $0 \le x < \frac{1}{4}$; $h(x) = \frac{1}{2}$, $\frac{1}{4} \le x < \frac{3}{4}$; $h(x) = \frac{1}{2} + 5(x - \frac{3}{4})^2$, $\frac{3}{4} \le x < 1$
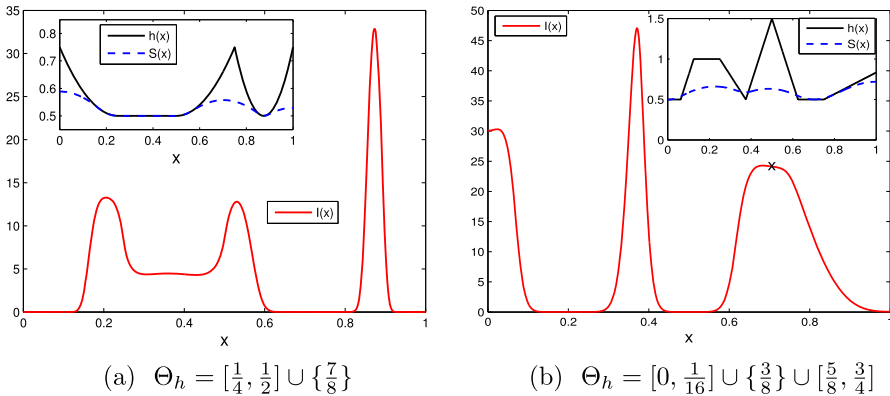

(a) $\Theta_h = [\frac{1}{4}, \frac{1}{2}] \cup \{\frac{7}{8}\}$ (b) $\Theta_h = [0, \frac{1}{16}] \cup \{\frac{3}{8}\} \cup [\frac{5}{8}, \frac{3}{4}]$

Fig. 5 Numerical simulations of the solution profile of model (1.6), where $d_S = 1$, $d_I = 10^{-5}$, $\beta(x) = 1 + \frac{1}{2}\sin(2\pi x)$, $\eta(x) = 1$, $\gamma(x) = h(x)\beta(x) - \eta(x)$, $\Lambda = 10$. In (**a**) and (**b**), $h(x)$ is chosen to be the same as $k(x)$ in Fig. 2b, c, respectively

following risk function whose curve is the connection of two segments:

$$h(x) = \begin{cases} a_1 \left(x - \frac{L}{2}\right) + \frac{\Lambda}{4}, \ x \in \left[0, \frac{L}{2}\right], \\ a_2 \left(x - \frac{L}{2}\right) + \frac{\Lambda}{4}, \ x \in \left(\frac{L}{2}, L\right], \end{cases} \tag{3.1}$$

with $a_1 < 0$, $a_2 > 0$. Obviously, h is merely Lipschitz continuous at $x = \frac{L}{2}$. Our numerical simulation results demonstrate that if the slopes $|a_1|$, a_2 are properly large, then the infected population will concentrate at $x = \frac{L}{2}$ (Fig. 6a); if $|a_1|$, a_2 are small, then the infected population will aggregate in a neighborhood of $x = \frac{L}{2}$ (Fig. 6b); and if $|a_1|$ is small while a_2 is large, then the infected population will aggregate in a left-neighborhood of $x = \frac{L}{2}$ (Fig. 6b). These profiles behave rather differently from that
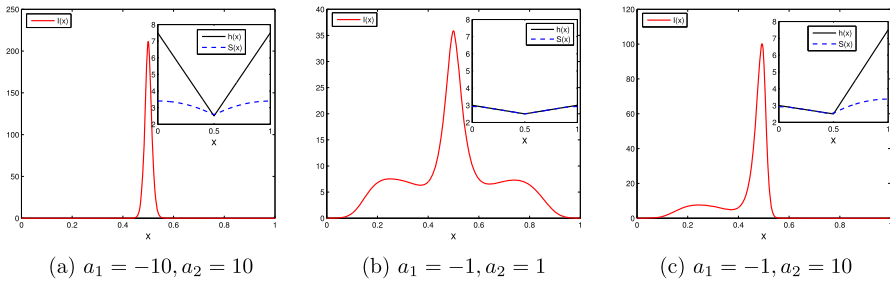
(a) $a_1 = -10, a_2 = 10$ (b) $a_1 = -1, a_2 = 1$ (c) $a_1 = -1, a_2 = 10$

Fig. 6 Numerical simulations of the solution profile of model (1.6), where $\beta(x) = 1 + \frac{1}{2}\sin(2\pi x)$, $\eta(x) = 1$, $\gamma(x) = h(x)\beta(x) - \eta(x)$, $L = 1$, $d_S = 1$, $d_I = 10^{-5}$, $\Lambda = 10$ and $h(x)$ is given by (3.1)

in Theorem 2.3(ii) for $h \in C^2([0, L])$, as shown by Fig. 4a. Therefore, the numerical results reveal that the smoothness of h may have a substantial affect on the spatial distribution of the disease. This observation implies that drastic changes in the spatial environment, such as the transmission, recovery or death rates, may have substantial effects on the distribution profiles of the disease in space.

3.3 Conclusion

The discussions in the above two subsections, together with the numerical simulations, show that the spatial profile of the susceptible and infected populations of (1.2) and (1.6) with respect to small movement rate of the infected individuals are rather different. This is caused by the presence of the recruitment term for the susceptible population and the death rate for the infected population. On the other hand, we would like to mention that the recent works (Cui 2021; Cui et al. 2017, 2021; Cui and Lou 2016; Kuto et al. 2017; Lei and Zhou 2022; Zhang and Cui 2020) studied various kinds of reaction–diffusion–advection SIS epidemic models, in which the advection term represents some passive movement in a certain direction, e.g., due to external environmental forces such as water flow and so on. In particular, if an advection is present in (1.2) and stands for, for instance, the water flow, it was proved in Cui et al. (2021, Theorem 1.4) that, as $d_I \to 0$, the susceptible population converges to a positive function while the infected population concentrates only at the downstream of the water flow; a similar result can be shown to hold for the corresponding system (1.6). Such a distribution behavior is essentially different from that of (1.2) and (1.6) with small d_I.

In summary, our results here, combined with those of Cui et al. (2021); Kuto et al. (2017); Li et al. (2018), suggest that the recruitment term for the susceptible population, the death rate for the infected population (even the smoothness of the associated risk function) as well as the advection can lead to significant impacts on the disease transmission and thus decision-makers should attach great importance to these factors when taking measures such as the lockdown and quarantine to control the movement or immigration of the infected individuals so as to eliminate the disease infection.

4 Proof of main results: Theorems 2.1, 2.2 and 2.3

This section is devoted to the proof of Theorems 2.1, 2.2 and 2.3.

4.1 Proof of Theorem 2.1

In this subsection, we present the proof of Theorem 2.1.

Proof of Theorem 2.1 First of all, we recall that for any EE (S, I) of (1.2), from Wen et al. (2018) (see (3.3) there), the following holds:

$$k_{min} \le S(x) \le \max_{[0,L]} k(x), \quad \forall x \in [0, L]. \tag{4.1}$$

By the positivity of I and the uniqueness of the principal eigenvalue, it is clear from the equation of I that

$$\lambda_1(d_I, \gamma - \beta S) = 0, \quad \forall d_I > 0,$$

where $\lambda_1(d_I, \gamma - \beta S)$ is defined as in the appendix. Using Theorem 1.1, as $d_I \to 0$ (up to a subsequence), we see that $S \to \hat{S}$ uniformly on $[0, L]$ for some positive function $\hat{S}$. Hence, by Lemma 5.1 in the appendix and the continuous dependence of the principal eigenvalue on the weight function $\gamma - \beta S$, we have

$$0 = \lim_{d_I \to 0} \lambda_1(d_I, \gamma - \beta S) = \min_{x \in [0,L]} [\gamma(x) - \beta(x)\hat{S}(x)].$$

This obviously implies that

$$\hat{S}(x) \le k(x), \quad \forall x \in [0, L] \text{ and } \hat{S}(y_0) = k(y_0) \tag{4.2}$$

for some $y_0 \in [0, L]$.

From Theorem 1.1, we recall that $I \to \mu$ weakly for some Radon measure μ with $\mu([0, L]) > 0$ in the following sense

$$\int_0^L I(x)\zeta(x)dx \to \int_0^L \zeta(x)\mu(dx), \quad \forall \zeta \in C([0, L]), \text{ as } d_I \to 0. \tag{4.3}$$

We now integrate the first equation in (1.2) by parts over $[0, L]$ and use the boundary conditions to deduce that

$$\int_0^L [\beta(x)S(x) - \gamma(x)]I(x)dx = 0, \quad \forall d_I > 0. \tag{4.4}$$

Letting $d_I \to 0$ in (4.4), combined with (4.3) and the fact that $S \to \hat{S}$ uniformly on $[0, L]$ as $d_I \to 0$, we infer that

$$\int_{[0,L]} [\beta(x)\hat{S}(x) - \gamma(x)]\mu(\mathrm{d}x) = 0, \tag{4.5}$$

which, together with (4.2), gives

$$\int_{\{x \in [0,L]: \, \hat{S}(x) < k(x)\}} \beta(x)[\hat{S}(x) - k(x)]\mu(\mathrm{d}x) = \int_{[0,L]} \beta(x)[\hat{S}(x) - k(x)]\mu(\mathrm{d}x) = 0.$$

As a result, we find that

$$\mu(\{x \in [0, L] : \, \hat{S}(x) < k(x)\}) = 0 \tag{4.6}$$

and

$$\mu(\{x \in [0, L] : \, \hat{S}(x) = k(x)\}) = \mu([0, L]) > 0. \tag{4.7}$$

In view of (4.4) and $\int_0^L (S(x) + I(x))\,\mathrm{d}x = N$, for any $d_I > 0$ we have

$$\int_0^L S(x)I(x)\mathrm{d}x \le \frac{1}{\min_{[0,L]} \beta(x)} \int_0^L \gamma(x)I(x)\mathrm{d}x \le \frac{\max_{[0,L]} \gamma(x)}{\min_{[0,L]} \beta(x)} N, \quad \forall d_I > 0. \tag{4.8}$$

Then, applying the L^1-theory for elliptic equation (see Lemma 5.2 in the appendix) to the S-equation, one sees that for any $1 \le r < \infty$,

$$\|S\|_{W^{1,r}(0,L)} \le C, \quad \forall d_I > 0. \tag{4.9}$$

Hereafter, C or $C(\epsilon)$ is a positive constant independent of $d_I > 0$ but may be different from place to place. Taking $r = 2$ in (4.9), we note that $W^{1,2}(0, L)$ is a Hilbert space and $W^{1,2}(0, L)$ is compactly embedded to $C([0, L])$. Thus, we may assume that $S \to \hat{S}$ weakly in $W^{1,2}(0, L)$ and $S \to \hat{S}$ uniformly on $[0, L]$ as $d_I \to 0$. Now, for any $\zeta \in W^{1,2}(0, L)$ (and so $\zeta \in C([0, L])$), we get from the S-equation that

$$d_S \int_0^L S_x(x)\zeta_x(x)\mathrm{d}x = \int_0^L [-\beta(x)S(x) + \gamma(x)]I(x)\zeta(x)\mathrm{d}x, \quad \forall d_I > 0. \tag{4.10}$$

By virtue of (4.3), (4.6) and (4.7), we can send $d_I \to 0$ in (4.10) to obtain

$$d_S \int_0^L \hat{S}_x(x)\zeta_x(x)\mathrm{d}x = 0, \quad \forall \zeta \in W^{1,2}(0, L).$$

This means that $\hat{S}$ is a weak (and then a classical) solution of

$$-u_{xx}(x) = 0, \quad x \in (0, L); \quad u_x(0) = u_x(L).$$

Consequently, $\hat{S}$ must be a positive constant. It then follows from (4.2) that $\hat{S} = k_{min}$, and so $S(x) \to k_{min}$ uniformly on $[0, L]$.

In the sequel, we are going to determine the limit of I. We first consider case (i): $\Theta_k = \{x_0\}$ is a singleton. By what was proved above, it is easily seen that

$$I(x) \to (N - Lk_{min})\delta(x_0) \quad \text{weakly in the sense of (1.3)},$$

where $\delta(x_0)$ is the Dirac measure centered at x_0.

It remains to show $I(x) \to 0$ locally uniformly in $[0, L] \setminus \{x_0\}$. We only consider the case of $x_0 \in (0, L)$, and the case $x_0 = 0$ or L can be handled similarly. Since $S(x) \to k_{min}$ uniformly on $[0, L]$, by the definition of k_{min}, we know from the I-equation that, given small $\epsilon > 0$, $I_{xx} > 0$ on $[0, x_0 - \epsilon] \cup [x_0 + \epsilon, L]$ as long as d_I is small enough. As $I_x(0) = I_x(L) = 0$, I is increasing in $[0, x_0 - \epsilon]$ while is decreasing in $[x_0 + \epsilon, L]$. Thus, due to the arbitrariness of ϵ, it readily follows from (4.6) that $I(x) \to 0$ locally uniformly in $[0, x_0) \cup (x_0, L]$, as claimed.

We next consider case (ii): $\Theta_k = [\varrho_1, \varrho_2] \subset (0, L)$. First of all, we can assert that $I(x) \to 0$ locally uniformly in $[0, L] \setminus [\varrho_1, \varrho_2]$ by a similar argument as in case (i). In what follows, we will analyze the limiting behavior of I in the interval $[\varrho_1, \varrho_2]$. To this end, let us introduce the following function

$$w(x) = \frac{S(x) - k_{min}}{d_I}, \quad x \in [0, L].$$

Due to (4.1), $w \geq 0$ on $[0, L]$. In addition, by our assumption, one notices that w solves

$$-d_S w_{xx}(x) = -\beta(x)Iw, \quad x \in [\varrho_1, \varrho_2], \tag{4.11}$$

and I satisfies

$$-I_{xx}(x) = \beta(x)wI, \quad x \in [\varrho_1, \varrho_2]. \tag{4.12}$$

Since $\int_0^L I(x)\mathrm{d}x \leq N$, for any small $\epsilon > 0$, Lemma 5.3(b) in the appendix can be applied to (4.11) to assert that

$$\max_{x \in [\varrho_1 + \epsilon, \varrho_2 - \epsilon]} w(x) \leq C(\epsilon) \min_{x \in [\varrho_1 + \epsilon, \varrho_2 - \epsilon]} w(x). \tag{4.13}$$

We now claim that w is uniformly bounded on $[\varrho_1 + \epsilon, \varrho_2 - \epsilon]$ for all small $d_I > 0$. Otherwise, there is a sequence of d_I, labelled by itself for simplicity, such that the

corresponding solution sequence $\{(w, I)\}$ satisfies

$$\max_{x \in [\varrho_1 + \epsilon, \varrho_2 - \epsilon]} w(x) \to \infty, \quad \text{as } d_I \to 0. \tag{4.14}$$

By (4.13), $w \to \infty$ uniformly on $[\varrho_1 + \epsilon, \varrho_2 - \epsilon]$ as $d_I \to 0$. To produce a contradiction, let us denote $\lambda_1^{\mathcal{D}}$ to be the principal eigenvalue of the following eigenvalue problem with Dirichlet boundary conditions:

$$\begin{cases} -\varphi_{xx} = \lambda \varphi, & x \in (\varrho_1 + \epsilon, \varrho_2 - \epsilon) \\ \varphi(\varrho_1 + \epsilon) = \varphi(\varrho_2 - \epsilon) = 0. \end{cases} \tag{4.15}$$

Apparently, $\lambda_1^{\mathcal{D}} > 0$. For all small $d_I > 0$, by (4.14) we may assume that

$$\beta(x)w(x) > 2\lambda_1^{\mathcal{D}} \quad \text{on } [\varrho_1 + \epsilon, \varrho_2 - \epsilon].$$

Thus, it follows from (4.12) that $I \in C^2([0, L])$ is a positive and strict supersolution of the following operator in the sense of Peng and Zhao (2015, Definition 2.1):

$$\begin{cases} \mathcal{L}u := -u_{xx} - 2\lambda_1^{\mathcal{D}}u, & x \in (\varrho_1 + \epsilon, \varrho_2 - \epsilon), \quad \forall u \in C^2([0, L]), \\ u(\varrho_1 + \epsilon) = u(\varrho_2 - \epsilon) = 0. \end{cases}$$

By means of Peng and Zhao (2015, Proposition 2.1) the principal eigenvalue, denoted by $\tilde{\lambda}_1^{\mathcal{D}}$, of the eigenvalue problem

$$\begin{cases} \mathcal{L}\varphi_{xx} = \lambda \varphi, & x \in (\varrho_1 + \epsilon, \varrho_2 - \epsilon), \\ \varphi(\varrho_1 + \epsilon) = \varphi(\varrho_2 - \epsilon) = 0 \end{cases}$$

satisfies $\tilde{\lambda}_1^{\mathcal{D}} > 0$.

On the other hand, the uniqueness of the principal eigenvalue of problem (4.15) implies $\tilde{\lambda}_1^{\mathcal{D}} + 2\lambda_1^{\mathcal{D}} = \lambda_1^{\mathcal{D}}$, and so $\tilde{\lambda}_1^{\mathcal{D}} = -\lambda_1^{\mathcal{D}} < 0$, leading to a contradiction. The previous claim is thus verified. Due to the arbitrariness of ϵ, we have shown that w is locally uniformly bounded in (ϱ_1, ϱ_2) with respect to all small $d_I > 0$.

Furthermore, by Lemma 5.2 in the appendix, it is easy to see from (4.12) that I is locally uniformly bounded in (ϱ_1, ϱ_2) independent of all small $d_I > 0$. The standard regularity theory for elliptic equations can be applied to (4.11) and (4.12), respectively to deduce that w and I are locally bounded (independent of small d_I) in (ϱ_1, ϱ_2) in the usual $C^{2+\alpha}$-norm for some $\alpha \in (0, 1)$. Then, by a diagonal argument, we may assume that

$$(w, I) \to (\hat{w}, \hat{I}) \quad \text{in } C^2_{loc}(\varrho_1, \varrho_2), \quad \text{as } d_I \to 0.$$

Clearly, by (4.12), $(\hat{w}, \hat{I})$ satisfies

$$-\hat{I}_{xx}(x) = \beta(x)\hat{w}\hat{I}, \quad x \in (\varrho_1, \varrho_2). \tag{4.16}$$

Furthermore, by adding (4.11) and (4.12), one easily sees that $(\hat{w}, \hat{I})$ solves

$$-(d_S\hat{w} + \hat{I})_{xx} = 0 \quad \text{in } (\varrho_1, \varrho_2).$$

This indicates that

$$d_S\hat{w}(x) + \hat{I}(x) = \hat{a} + \hat{b}x, \quad x \in (\varrho_1, \varrho_2) \tag{4.17}$$

for some constants $\hat{a}$, $\hat{b}$.

In what follows, we aim to determine $\hat{a}$ and $\hat{b}$. By a simple observation, (w, I) satisfies

$$\begin{cases} -(d_Sw + I)_{xx} = 0, & x \in (0, L), \\ (d_Sw + I)_x = 0, & x = 0, L. \end{cases}$$

Thus, $d_Sw + I = c_{d_I}$ is a positive constant on $[0, L]$ for any $d_I > 0$. Recall that w, I are locally uniformly bounded in (ϱ_1, ϱ_2). Hence, as $d_I \to 0$, we may assume that

$$d_Sw + I = c_{d_I} \to \hat{c} \in [0, \infty) \quad \text{uniformly on } [0, L].$$

From (4.17) it follows that $\hat{c} = \hat{a}$ and $\hat{b} = 0$. In addition, our analysis indicates that w and I are uniformly bounded on $[0, L]$. Precisely, it holds that

$$w(x), \quad I(x) \leq C, \quad \forall x \in [0, L]. \tag{4.18}$$

We now use the equation of I, together with the fact of w, $I \geq 0$ and the definition of k, to find that

$$\begin{aligned} -I_{xx} &= \frac{\beta(x)\,[S - k(x)]\,I}{d_I} \\ &= \beta(x) \left[\frac{S - k_{min}}{d_I} + \frac{k_{min} - k(x)}{d_I} \right] I \\ &\leq \beta(x)wI, \quad x \in (0, L). \end{aligned} \tag{4.19}$$

Multiplying both sides in (4.19) by I and integrating over $(0, L)$, we obtain

$$\int_0^L (I_x)^2 \mathrm{d}x \leq \int_0^L \beta w I^2 \mathrm{d}x \leq C$$

due to (4.18). This and (4.18) imply that $\|I\|_{W^{1,2}(0,L)} \leq C$. Since $W^{1,2}(0, L)$ is compactly embedded to $C([0, L])$, we can assume that $I \to \hat{I}$ uniformly on $[0, L]$. By what was proved before, $\hat{I} = 0$ on $[0, \varrho_1] \cup [\varrho_2, L]$, and by (4.16) and (4.17), on

$[\varrho_1, \varrho_2]$, $\hat{I}$ solves

$$\begin{cases} -\hat{I}_{xx} = \frac{\beta(x)}{d_S}(\hat{a} - \hat{I})\hat{I}, & \varrho_1 < x < \varrho_2, \\ \hat{I} = 0, & x = \varrho_1, \varrho_2. \end{cases} \tag{4.20}$$

Because of $\int_0^L (S(x) + I(x))\,dx = N$ and $S \to k_{min}$ uniformly on $[0, L]$ as $d_I \to 0$, it is easily seen that

$$\int_{\varrho_1}^{\varrho_2} \hat{I}\,dx = N - Lk_{min} > 0. \tag{4.21}$$

Thanks to the Harnack inequality (see Lemma 5.3(b)) and (4.21), we have from (4.20) that $\hat{I} > 0$ in (ϱ_1, ϱ_2). By (4.17) and the fact of $\hat{b} = 0$, clearly $\hat{a} > 0$.

It is well known that given $\hat{a} > 0$, the positive solution of problem (4.20), if it exists, must be unique, denoted by $\hat{I}_{\hat{a}}$; moreover, if $0 < \hat{a}_1 < \hat{a}_2$, then $\hat{I}_{\hat{a}_1}(x) < \hat{I}_{\hat{a}_2}(x)$ for all $x \in (\varrho_1, \varrho_2)$. With these facts, one can check that the positive constant $\hat{a}$ is uniquely determined by (4.21) in an implicit manner. Therefore, all the assertions in case (ii) have been verified. The proof is thus complete. □

4.2 Proof of Theorem 2.2

We are now in a position to give the proof of Theorem 2.2.

Proof of Theorem 2.2 First of all, one can follow the analysis of Theorem 2.1, combined with the result of Theorem 1.2 and its proof (see Li et al. 2018, Theorem 3.2), to show that as $d_I \to 0$, any EE (S, I) of (1.6) satisfies (up to a subsequence of d_I) that $S \to \hat{S}$ weakly in $W^{1,2}(0, L)$ and uniformly on $[0, L]$, and $I \to \mu$ weakly in the sense of (1.3) for some Radon measure μ and positive function $\hat{S} \in W^{1,2}(0, L)$, and

$$0 < \hat{S}(x) \le h(x), \quad \forall x \in [0, L], \tag{4.22}$$

and (2.5) hold.

For any $\zeta \in W^{1,2}(0, L)$ (and so $\zeta \in C([0, L])$), we use the S-equation to obtain

$$d_S \int_0^L S_x \zeta_x \, dx = \int_0^L [\Lambda - S - \beta(x)SI + \gamma(x)I]\zeta \, dx$$
$$= \int_0^L [\Lambda - S - \eta(x)I]\zeta \, dx - \int_0^L [\beta(x)S - (\gamma(x) + \eta(x))]I\zeta \, dx \tag{4.23}$$

for all $d_I > 0$. In view of (4.22) and (2.5), we send $d_I \to 0$ to infer that

$$\int_0^L [\beta(x)S - (\gamma(x) + \eta(x))]I\zeta \, dx \to \int_{[0,L]} \beta(x)[\hat{S} - h(x)]\zeta \mu(dx) = 0.$$

Thus, by letting $d_I \to 0$, it follows from (4.23) that

$$d_S \int_0^L \hat{S}_x \zeta_x dx = \int_0^L (\Lambda - \hat{S}) \zeta \, dx - \int_0^L \eta(x) \zeta \mu(dx), \quad \forall \zeta \in W^{1,2}(0, L).$$

(4.24)

Together with (2.5), this means that $\hat{S} \in W^{1,2}(0, L)$ is a weak solution of (2.4).

In what follows, for a general positive Hölder continuous function h, we will prove three claims:

Claim 1. If the minimum of h is attained at $x = 0$ (resp. at $x = L$), then $\hat{S}$ must touch h at this point; that is, $\hat{S}(0) = h(0) = h_{min}$ (resp. $\hat{S}(L) = h(L) = h_{min}$).

We only handle the case that h_{min} is attained at $x = 0$, and the other case can be treated similarly. Since $\hat{S} \leq h$ on $[0, L]$, we suppose that $\hat{S}(0) < h(0)$ and so $\hat{S}(x) < h(x)$ on $[0, \epsilon_0]$ for some small $\epsilon_0 > 0$. Thus, from (2.4), we have $-d_S \hat{S}_{xx} = \Lambda - \hat{S}$, $\forall x \in (0, \epsilon_0]$. A simple analysis shows that

$$\hat{S}(x) = c_1 e^{d_S^{-1/2} x} + c_2 e^{-d_S^{-1/2} x} + \Lambda, \quad x \in (0, \epsilon_0]$$

(4.25)

for some constants c_1, c_2. On the other hand, using the S-equation, we integrate on $[0, x]$ to deduce

$$- S_x(x) = \frac{1}{d_S} \int_0^x [\Lambda - S(y) - \beta(y)S(y)I(y) + \gamma(y)I(y)] dy, \quad x \in [0, \epsilon_0].$$

(4.26)

From the proof of Li et al. (2018, Theorem 3.2) we know that

$$\int_0^L S(x)I(x)dx \leq C, \quad \int_0^L I(x)dx \leq C, \text{ and } S(x) \leq C, \quad \forall x \in [0, L],$$

(4.27)

for some positive constant C, independent of $d_I > 0$.

In the sequel, the constant C allows to vary from line to line but does not depend on $d_I > 0$. It immediately follows from (4.26) that S_x is uniformly bounded on $[0, \epsilon_0]$, independent of $d_I > 0$. Note that $\mu([0, \epsilon_0]) = 0$ due to (2.5), and $I \to \mu$ weakly in the sense of (1.3). Given any small $\epsilon > 0$, we can find a small $\rho > 0$ so that for all $0 < d_I \leq \rho$,

$$\int_0^{\epsilon_0} I(x)dx \leq \epsilon + \int_{[0,\epsilon_0]} \mu(dx) = \epsilon.$$

Now, for any x_1, $x_2 \in [0, \epsilon_0]$ satisfying $|x_1 - x_2| < \epsilon$, we have

$$
\begin{aligned}
\left| S_x(x_1) - S_x(x_2) \right| &= \frac{1}{d_S} \left| \int_{x_1}^{x_2} [\Lambda - S(y) - \beta(y)S(y)I(y) + \gamma(y)I(y)] dy \right| \\
&\leq C|x_1 - x_2| + C \int_{x_1}^{x_2} I(y) dy \\
&\leq C|x_1 - x_2| + C \int_0^{\epsilon_0} I(y) dy \leq C\epsilon
\end{aligned}
$$

provided that $0 < d_I \leq \rho$. This shows that S_x is equi-continuous on $[0, \epsilon_0]$ once $0 < d_I \leq \rho$.

Hence, we can apply the well-known Ascoli-Arzelà theorem, up to a further subsequence of d_I, to conclude that S_x is uniformly convergent on $[0, \epsilon_0]$ as $d_I \to 0$. As

$$
S(x) - S(0) = \int_0^x S_x(y) dy, \quad S \to \hat{S} \text{ uniformly on } [0, \epsilon_0],
$$

it is easily seen that $S \to \hat{S}$ in $C^1([0, \epsilon_0])$. Thus, $\hat{S}_x(0) = 0$, and in turn we get from (4.25) that $c_1 = c_2$. Because of $\hat{S} \leq h$ on $[0, L]$ and the condition (2.3), we have $c_1 = c_2 < 0$, and so

$$
\hat{S}_x(x) = c_1[e^{d_S^{-1/2}x} - e^{-d_S^{-1/2}x}] < 0, \quad \forall x \in (0, \epsilon_0].
$$

This means that $\hat{S}$ is decreasing on $[0, \epsilon_0]$.

By virtue of $h(0) \leq h(x)$ for all $x \in [0, L]$ and (2.5), one can extend the above analysis to assert that $\hat{S}$ is decreasing on $[0, L]$ and so $\hat{S} < h$ on $[0, L]$. This clearly gives $\mu([0, L]) = 0$, a contradiction with $\mu([0, L]) > 0$ due to (2.5) again. Hence, we must have $\hat{S}(0) = h(0) = h_{min}$.

Claim 2. If $\hat{S}$ attains its local minimum at some $x_0 \in (0, L)$, then $\hat{S}$ must touch h at this point; that is, $\hat{S}(x_0) = h(x_0)$.

Suppose that $\hat{S}(x_0) < h(x_0)$ due to $\hat{S} \leq h$. Thus, there is a small $\epsilon_0 > 0$ such that $\hat{S}(x) < h(x)$ for all $x \in [x_0 - \epsilon_0, x_0 + \epsilon_0] \subset (0, L)$. By (2.5), $\mu([x_0 - \epsilon_0, x_0 + \epsilon_0]) = 0$ and so

$$
-d_S \hat{S}_{xx} = \Lambda - \hat{S} \quad \text{on } [x_0 - \epsilon_0, x_0 + \epsilon_0].
$$

As before, $\hat{S}$ takes the form of (4.25) on $[x_0 - \epsilon_0, x_0 + \epsilon_0]$ for some constants c_1, c_2. Obviously, $\hat{S}_x(x_0) = 0$, which leads to $c_2 = c_1 e^{2d_S^{-1/2}x_0}$, and so $c_1 < 0$. Thus, it holds that

$$
\hat{S}(x) = c_1[e^{d_S^{-1/2}x} + e^{d_S^{-1/2}(2x_0 - x)}] + \Lambda, \quad x \in [x_0 - \epsilon_0, x_0 + \epsilon_0] \qquad (4.28)
$$

for some constant $c_1 < 0$. In view of (4.28), basic computation gives that $\hat{S}$ is increasing on $[x_0 - \epsilon_0, x_0]$ while is decreasing on $[x_0, x_0 + \epsilon_0]$. This implies that x_0 is a local

maximum of $\hat{S}$, a contradiction with our assumption. As a result, $\hat{S}$ must touch h at $x = x_0$.

Claim 3. If the minimum of h is attained at some point $y_0 \in (0, L)$, then $\hat{S}$ must touch h at this point; that is, $\hat{S}(y_0) = h(y_0) = h_{min}$.

Suppose that $\hat{S}(y_0) < h(y_0) = h_{min}$. There are two possible cases to happen in the interval $[0, y_0]$: Case 1. $\hat{S}$ never touches h in $[0, y_0)$, that is, $\hat{S} < h$ in $[0, y_0)$; Case 2. $\hat{S}$ touches h somewhere in $[0, y_0)$.

When Case 1 occurs, by (2.5), we know that $\hat{S}$ must touch h in $(y_0, L]$. Let y_1 be the first point (from the left side) at which $\hat{S}$ touches h. That is, $y_1 \in (y_0, L]$, and

$$\hat{S}(x) < h(x), \quad \forall x \in (y_0, y_1), \quad \hat{S}(y_1) = h(y_1) \geq h_{min}.$$

On the other hand, since $\hat{S} < h$ in $[0, y_0)$, we can follow the analysis used in **Claim 1** to show that $\hat{S}$ is decreasing on $[0, y_1]$. This is an obvious contradiction with $\hat{S}(y_0) < h_{min} \leq \hat{S}(y_1)$.

When Case 2 occurs, we denote by $y_2 \in [0, y_0)$ the first point from the right side such that $\hat{S}$ touches h in $[0, y_0)$. That is,

$$\hat{S}(x) < h(x), \quad \forall x \in (y_2, y_0), \quad \hat{S}(y_2) = h(y_2) \geq h_{min}.$$

If $\hat{S}$ does not touch h in $(y_0, L]$. By a similar argument to the proof of **Claim 1** and appealing to the fact of $S_x(L) = 0$, one sees that $\hat{S}$ is increasing in $(y_2, L]$, leading to $\hat{S}(y_2) < \hat{S}(y_0)$, which contradicts with $\hat{S}(y_2) \geq h_{min} > \hat{S}(y_0)$. Hence, it is necessary that $\hat{S}$ touches h in $(y_0, L]$. Let y_3 be the first point where $\hat{S}$ touches h in $(y_0, L]$. Thus, $\hat{S}(x) < h(x)$ for all $x \in (y_0, y_3)$ and $\hat{S}(y_3) = h(y_3) \geq h_{min}$. Therefore, $\hat{S}(x) < h(x)$ in the interval (y_2, y_3), $\hat{S}(y_0) < h(y_0) = h_{min}$ and $\hat{S}(y_2)$, $\hat{S}(y_3) \geq h_{min}$. This implies that on $[y_2, y_3]$, $\hat{S}$ must attain its minimum at some $y_4 \in (y_2, y_3)$. By **Claim 2**, we can conclude that $\hat{S}(y_4) = h(y_4)$, a contradiction again. So far, we have verified **Claim 3**.

A similar reasoning as that of proving **Claim 3** yields $\hat{S} \geq h_{min}$ on $[0, L]$. Thus (2.6) holds. Thanks to **Claim 1** and **Claim 3**, (2.7) is true. It is also apparent that **Claim 2** implies (2.8). The proof is now complete. □

4.3 Proof of Theorem 2.3

This subsection is devoted to the proof of Theorem 2.3. We begin with some lemmas as follows.

Lemma 4.1 *Assume that $h \in C^2([0, L])$ and h_x is non-decreasing in some neighborhood of $\varrho_0 \in \Theta_h$. Let $\hat{S}$ and μ be given as in Theorem 2.2. Then there exists a small $\epsilon_0 > 0$ such that*

$$\hat{S}(x) = h(x), \quad \forall x \in (\varrho_0 - \epsilon_0, \varrho_0 + \epsilon_0) \cap (0, L)$$

and

$$\mu(\{x\}) = \frac{\Lambda - h + d_S h_{xx}}{\eta(x)}, \quad \text{a.e. for } x \in (\varrho_0 - \epsilon_0, \varrho_0 + \epsilon_0) \cap (0, L).$$

Proof By Theorem 2.2, we know that $\varrho_0 \in \{x \in [0, L] : \hat{S}(x) = h(x)\}$. In the sequel, we only consider the case of $\varrho_0 \in (0, L)$, and the case of $\varrho_0 = 0$ or L can be treated similarly. There are three possibilities we have to distinguish:

(1) ϱ_0 is an isolated point in the set $\{x \in [0, L] : \hat{S}(x) = h(x)\}$;

(2) ϱ_0 is an accumulation point in $\{x \in [0, L] : \hat{S}(x) = h(x)\}$;

(3) there is a small $\epsilon_0 > 0$ such that $(\varrho_0 - \epsilon_0, \varrho_0 + \epsilon_0) \subset \{x \in [0, L] : \hat{S}(x) = h(x)\}$.

In what follows, we will exclude (1) and (2). If (1) happens, then

$$\hat{S}(\varrho_0) = h(\varrho_0) = h_{min} \text{ and } \hat{S} < h \text{ in } (\varrho_0 - \epsilon_1, \varrho_0 + \epsilon_1) \setminus \{\varrho_0\}$$

for some small $\epsilon_1 > 0$.

Note that $\mu([0, L]) < \infty$. In view of this fact, one can apply the interior regularity theory for elliptic equations to (2.4) and assert that $\hat{S} \in C^1(0, L)$. Clearly, $h_x(\varrho_0) = 0$. Since $\hat{S}(\varrho_0) = h(\varrho_0) = h_{min}$ and $\hat{S} \geq h_{min}$ due to (2.6), we infer that $\hat{S}_x(\varrho_0) = 0$.

On the other hand, by (2.4), $\hat{S}$ satisfies

$$- d_S \hat{S}_{xx} = \Lambda - \hat{S} \quad \text{in } (\varrho_0 - \epsilon_1, \varrho_0 + \epsilon_1) \setminus \{\varrho_0\}. \tag{4.29}$$

By using $\hat{S}_x(\varrho_0) = 0$ and (4.29), one can easily see that $\hat{S}$ is increasing in $(\varrho_0 - \epsilon_1, \varrho_0)$ while $\hat{S}$ is decreasing in $(\varrho_0, \varrho_0 + \epsilon_1)$. This implies that $\hat{S} < h_{min}$ in $(\varrho_0 - \epsilon_1, \varrho_0 + \epsilon_1) \setminus \{\varrho_0\}$, contradicting against (2.6). Thus, (1) is impossible.

If (2) happens, without loss of generality, we can find two points, say z_1, z_2 with $\varrho_0 < z_1 < z_2 < \varrho_0 + \epsilon_2$ for some small $\epsilon_2 > 0$ such that

$$\hat{S}(z_1) = h(z_1), \quad \hat{S}(z_2) = h(z_2) \text{ and } \hat{S} < h \text{ in } (z_1, z_2). \tag{4.30}$$

By taking ϵ_2 to be smaller if necessary, we may assume that $h_x(z_1) \leq h_x(z_2)$ due to the monotonicity of h_x. Then, $\hat{S}$ solves (4.29) in (z_1, z_2). By means of (4.30), we have

$$\hat{S}_x(z_1) \leq h_x(z_1), \quad \hat{S}_x(z_2) \geq h_x(z_2),$$

leading to $\hat{S}_x(z_1) \leq \hat{S}_x(z_2)$. However, it follows from (4.29) that $\hat{S}_{xx} < 0$ in (z_1, z_2), which gives $\hat{S}_x(z_1) > \hat{S}_x(z_2)$, a contradiction. Hence, the possibility (2) has been ruled out.

The above argument shows that (3) must hold. Now, since $\hat{S} = h$ on $[\varrho_0 - \epsilon_0, \varrho_0 + \epsilon_0]$, we can multiply both sides of (2.5) by any function $\zeta \in C^2([0, L])$ with compact support on $[\varrho_0 - \epsilon_0, \varrho_0 + \epsilon_0]$ and integrate to conclude that

$$d_S h_{xx} + \Lambda - h - \eta(x)\mu(\{x\}) = 0, \quad \text{a.e. for } x \in (\varrho_0 - \epsilon_0, \varrho_0 + \epsilon_0),$$

which yields the expression of $\mu(\{x\})$.   □

Lemma 4.2 *Assume that $h \in C^2([0, L])$, h_x is non-decreasing on $[0, L]$, and $\Theta_h = \{\tau_0\}$ for some $\tau_0 \in (0, L)$. Then there exist two numbers τ_1, τ_2 with $0 < \tau_1 < \tau_0 < \tau_2 < L$ such that*

$$\hat{S}(x) = h(x), \quad \forall x \in [\tau_1, \tau_2], \tag{4.31}$$

and on $[0, \tau_1) \cup (\tau_2, L]$, $\hat{S}$ satisfies

$$\begin{cases} -d_S \hat{S}_{xx}(x) = \Lambda - \hat{S}, & x \in (0, \tau_1) \cup (\tau_2, L), \\ \hat{S}_x(0) = \hat{S}_x(L) = 0, \\ \hat{S}(\tau_1) = h(\tau_1), \quad \hat{S}(\tau_2) = h(\tau_2), \end{cases} \tag{4.32}$$

and μ satisfies

$$\mu(\{x\}) = \frac{\Lambda - h + d_S h_{xx}}{\eta(x)}, \quad \text{a.e. for } x \in (\tau_1, \tau_2), \tag{4.33}$$

$$\mu(\{x\}) = 0, \quad \forall x \in [0, \tau_1) \cup (\tau_2, L]. \tag{4.34}$$

Proof Let us denote

$$\tau_1 = \inf\{\tau \in [0, \tau_0) : \quad \hat{S}(x) = h(x), \ \forall x \in [\tau, \tau_0]\},$$
$$\tau_2 = \sup\{\tau \in (\tau_0, L] : \quad \hat{S}(x) = h(x), \ \forall x \in [\tau_0, \tau]\}.$$

Lemma 4.1 implies that τ_1 and τ_2 are well defined, and $0 \le \tau_1 < \tau_0$ and $\tau_0 < \tau_2 \le L$. In addition, (4.31) and (4.33) hold.

In light of the monotonicity of h_x on $[0, L]$, it is easily seen from the proof of Lemma 4.1 that if $\tau_1 > 0$, then $\hat{S}$ can not touch h in $(0, \tau_1)$ and in turn $\mu([0, \tau_1)) = 0$; similarly, if $\tau_2 < L$, $\hat{S}$ can not touch h in (τ_2, L) and so $\mu((\tau_2, L]) = 0$.

If $\tau_1 > 0$ and $\tau_2 < L$, we can use the analysis as in the proof of Claim 1 of Theorem 2.2 to conclude that $\hat{S}_x(0) = \hat{S}_x(L) = 0$. As $\mu([0, \tau_1) \cup (\tau_2, L]) = 0$, by (2.4) and the continuity of $\hat{S}$, a standard compactness argument of elliptic equations yields that $\hat{S}$ solves (4.32) in the classical sense. Clearly, the solution of (4.32) is unique.

It remains to prove $\tau_1 > 0$ and $\tau_2 < L$. Note that the monotonicity of h_x, $\Theta_h = \{\tau_0\}$ and $h_x(\tau_0) = 0$ ensure $h_x(0) < 0$ and $h_x(L) > 0$. Suppose that $\tau_1 = 0$, and so (4.31) holds on $[0, \tau_2]$. Now, given $\tau \in (0, \tau_0]$, integrating the S-equation over $[0, \tau]$ and using (4.31), we infer that

$$-d_S S_x(\tau^-) = \int_0^\tau [\Lambda - S(y) - \beta(y)S(y)I(y) + \gamma(y)I(y)]\mathrm{d}y$$

$$= \int_0^\tau [\Lambda - S(y) - \eta(y)I(y)]\mathrm{d}y$$

$$+ \int_0^\tau [\gamma(y) + \eta(y) - \beta(y)S(y)]I(y)\mathrm{d}y$$

$$\to \int_{[0,\tau]} [\Lambda - h(y) - \eta(y)\mu](\mathrm{d}y) = \int_0^\tau [-d_S h_{xx}(y)]\mathrm{d}y$$

$$= -d_S h_x(\tau) + d_S h_x(0), \quad \text{as } d_I \to 0.$$

That is, for any $\tau \in (0, \tau_0]$, it holds that

$$S_x(\tau^-) \to h_x(\tau) - h_x(0), \quad \text{as } d_I \to 0.$$

Since h_x is non-decreasing on $[0, \tau_0]$ and $h_x(0) < 0$, there exists a small $\epsilon_0 > 0$ such that for all $x \in [\tau_0 - \epsilon_0, \tau_0]$,

$$S_x(x^-) \geq \frac{1}{2}[h_x(\tau_0) - h_x(0)] = -\frac{1}{2}h_x(0) > 0$$

for all small $d_I > 0$. This implies that S is increasing on $[\tau_0 - \epsilon_0, \tau_0]$ for all such small $d_I > 0$. In view of $S \to h$ uniformly on $[\tau_0 - \epsilon_0, \tau_0]$ as $d_I \to 0$, h must be non-decreasing on $[\tau_0 - \epsilon_0, \tau_0]$, which is a contradiction against our assumption. Hence, $\tau_1 > 0$. Similarly, we have $\tau_2 < L$ by using $h_x(L) > 0$. As a consequence, we deduce (4.34). The proof is complete. □

Similar to the argument of Lemma 4.1, we can conclude the following result.

Lemma 4.3 *Assume that $h \in C^2([0, L])$, $[\varrho_1, \varrho_2] \subset \Theta_h$ and h_x is non-decreasing in some neighborhood of ϱ_1, ϱ_2. Let $\hat{S}$ and μ be given as in Theorem 2.2. Then there exists a small $\epsilon_0 > 0$ such that*

$$\hat{S}(x) = h(x), \quad \forall x \in (\varrho_1 - \epsilon_0, \varrho_2 + \epsilon_0) \cap (0, L)$$

and

$$\mu(\{x\}) = \frac{\Lambda - h + d_S h_{xx}}{\eta(x)}, \quad a.e. \text{ for } x \in (\varrho_1 - \epsilon_0, \varrho_2 + \epsilon_0) \cap (0, L).$$

Based upon Lemma 4.3, we can deduce the following result.

Lemma 4.4 *Assume that $h \in C^2([0, L])$, $\Theta_h = [\varrho_1, \varrho_2]$ and h_x is non-decreasing on $[0, \varrho_1] \cup [\varrho_2, L]$. Let $\hat{S}$ and μ be given as in Theorem 2.2. Then there exist two numbers τ_1, τ_2 with $0 < \tau_1 < \varrho_1 < \varrho_2 < \tau_2 < L$ such that all the assertions in Lemma 4.2 hold.*

With the aid of Lemmas 4.1–4.4, we are now in a position to prove Theorem 2.3.

Proof of Theorem 2.3 We first prove (i). We proceed indirectly and suppose that $\hat{S} \not\equiv h$ on $[0, L]$. Since $\hat{S}$ touches h at least at the highest-risk point due to Theorem 2.2, we can find an interval, denoted by $[\ell_1, \ell_2] \subset [0, L]$, such that $\hat{S} < h$ in (ℓ_1, ℓ_2) and at the boundary point $x = \ell_i$ for $i = 1, 2$, either $\hat{S}$ touches h (and so $\hat{S}(\ell_i) = h(\ell_i)$) or $\hat{S}(\ell_i) < h(\ell_i)$. In the latter case, it is necessary that $\ell_i = 0$ or L, and the analysis to deduce Claim 1 in the proof of Theorem 2.2 shows that $\hat{S}_x(\ell_i) = 0$. In any case, clearly $\hat{S}$ satisfies

$$\begin{cases} -d_S \hat{S}_{xx} = \Lambda - \hat{S}, & x \in (\ell_1, \ell_2), \\ \hat{S}(\ell_i) = h(\ell_i) \ \text{ or } \ \hat{S}_x(\ell_i) = 0, & i = 1, 2. \end{cases} \tag{4.35}$$

Thus, by our assumption, h is a sub-solution to problem (4.35), and $\max\{\Lambda, \ \max_{x \in [0,L]} h(x)\}$ is a super-solution to (4.35). The well-known technique of sub-supersolution iteration, combined with the uniqueness of solutions to problem (4.35), allows us to conclude that $\hat{S} \geq h$ on $[\ell_1, \ell_2]$, which leads to a contradiction. Hence, (2.9) holds, and (2.10) follows from (2.4) by using a test-function argument similarly as before. Therefore, (i) is proved.

We next prove (ii). First of all, let us consider the case of $\tau_0 \in (0, L)$. In this case, the assertions (2.11)-(2.14) follow from Lemma 4.2, and it remains to show that $\tau_1, \ \tau_2$ are uniquely determined by (2.15). As $\hat{S} < h$ in $[0, \tau_1)$, we have

$$\hat{S}(x) = c_1 [e^{d_S^{-1/2} x} + e^{-d_S^{-1/2} x}] + \Lambda, \quad \forall x \in [0, \tau_1]$$

for some $c_1 < 0$. It then follows from $\hat{S}(\tau_1) = h(\tau_1)$ that

$$\hat{S}(x) = -\frac{\Lambda - h(\tau_1)}{e^{d_S^{-1/2} \tau_1} + e^{-d_S^{-1/2} \tau_1}} (e^{d_S^{-1/2} x} + e^{-d_S^{-1/2} x}) + \Lambda, \quad \forall x \in [0, \tau_1].$$

Note that $\hat{S}$ is convex while h is concave in the interval $[0, \tau_1)$, and moreover, $\hat{S} \in C^1([0, L])$ as shown before. Hence, $\hat{S}$ must be tangent to h at $x = \tau_1$, which in turn implies that τ_1 is the unique solution to $\hat{S}_x(\tau_1) = h_x(\tau_1)$. Thus, τ_1 is uniquely determined by the following equation:

$$\frac{e^{d_S^{-1/2} \tau_1} - e^{-d_S^{-1/2} \tau_1}}{e^{d_S^{-1/2} \tau_1} + e^{-d_S^{-1/2} \tau_1}} = -\frac{d_S^{1/2} h_x(\tau_1)}{\Lambda - h(\tau_1)}.$$

Similarly, τ_2 is uniquely determined by the second equation of (2.15). The assertions in (ii)-(a) have been verified.

We now consider the case of $\tau_0 = L$. In view of our assumption, clearly $h_x(0) < 0$, $h_x(L) \leq 0$, and $\hat{S}(L) = h(L)$.

Assume that

$$\frac{e^{2L d_S^{-1/2}} - 1}{e^{2L d_S^{-1/2}} + 1} > -\frac{d_S^{1/2} h_x(L)}{\Lambda - h(L)}.$$

In order to deduce the desired conclusion in (ii)-(b1), one can follow the analysis of Lemmas 4.1 and 4.2. By checking the analysis there, one just needs to show that τ_1 defined in the assertion (ii)-(a) satisfies $\tau_1 > 0$. It turns out that this amounts to rule out the situation that $\hat{S} < h$ in $[0, L)$. Suppose that $\hat{S} < h$ in $[0, L)$. Then, arguing as before, we see that $\hat{S}$ satisfies $-d_S \hat{S}_{xx} = \Lambda - \hat{S}$ in $(0, L)$ and $\hat{S}_x(0) = 0$. Solving this problem, we get

$$\hat{S}(x) = c_1[e^{d_S^{-1/2}x} + e^{-d_S^{-1/2}x}] + \Lambda$$

for some $c_1 < 0$. It then follows from $\hat{S}(L) = h(L)$ that

$$c_1 = -\frac{\Lambda - h(L)}{e^{d_S^{-1/2}L} + e^{-d_S^{-1/2}L}}.$$

Thus, we get

$$\hat{S}_x(L) = -d_S^{-1/2}(\Lambda - h(L))\frac{e^{2Ld_S^{-1/2}} - 1}{e^{2Ld_S^{-1/2}} + 1}.$$

By means of $\hat{S} < h$ in $[0, L)$ and $\hat{S}(L) = h(L)$, it is necessary that $\hat{S}_x(L) \geq h_x(L)$, which leads to

$$\frac{e^{2Ld_S^{-1/2}} - 1}{e^{2Ld_S^{-1/2}} + 1} \leq -\frac{d_S^{1/2}h_x(L)}{\Lambda - h(L)},$$

contradicting with our assumption. Therefore, $\tau_1 > 0$ must hold, and (ii)-(b1) is proved.

Assume from now on that

$$\frac{e^{2Ld_S^{-1/2}} - 1}{e^{2Ld_S^{-1/2}} + 1} \leq -\frac{d_S^{1/2}h_x(L)}{\Lambda - h(L)}.$$

We first show that $\tau_1 > 0$ is impossible. On the contrary, we suppose that $\tau_1 > 0$, and by the above analysis, τ_1 must solve the first equation of (2.15). Let us consider the following auxiliary problem:

$$f(\tau) = \frac{e^{2\tau d_S^{-1/2}} - 1}{e^{2\tau d_S^{-1/2}} + 1} + \frac{d_S^{1/2}h_x(\tau)}{\Lambda - h(\tau)}, \quad \tau \in [0, L].$$

Since $h_x(\tau)$ is non-decreasing, $h_x(\tau) \leq 0$ on $[0, L]$, $h(\tau)$ is non-increasing and $h(\tau) > \Lambda$ on $[0, L]$, it is easy to check that $\frac{d_S^{1/2}h_x(\tau)}{\Lambda - h(\tau)}$ is non-decreasing on $[0, L]$. Clearly, $\frac{e^{2\tau d_S^{-1/2}} - 1}{e^{2\tau d_S^{-1/2}} + 1}$ is increasing on $[0, L]$. Therefore, $f(\tau)$ is increasing on $[0, L]$.

Observe that

$$f(L) = \frac{e^{2Ld_S^{-1/2}} - 1}{e^{2Ld_S^{-1/2}} + 1} + \frac{d_S^{1/2}h_x(L)}{\Lambda - h(L)} \le 0$$

due to our assumption. This implies that the first equation of (2.15) has no solution with respect to τ_1 in $[0, L)$, arriving at a contradiction. Hence, $\hat{S} < h$ in $[0, L)$ and $\mu([0, L)) = 0$, and so $\hat{S}$ solves (2.17). It remains to prove (2.18). Indeed, by integrating the sum of (1.6), we obtain

$$\Lambda L - \int_0^L S(x)\mathrm{d}x = \int_0^L \eta(x)I(x)\mathrm{d}x, \ \ \forall d_I > 0.$$

Letting $d_I \to 0$ yields

$$\Lambda L - \int_0^L \hat{S}(x)\mathrm{d}x = \int_{[0,L]} \eta(x)\mu(\mathrm{d}x) = \eta(L)\mu(\{L\}).$$

Here we used the fact of $\mu([0, L)) = 0$. This gives (2.18), and thus the assertions in (ii)-(b2) hold true.

The case of $\tau_0 = 0$ can be treated similarly as above. In view of Lemma 4.4 and the analysis above, the assertions in (iii) follow immediately. The proof is completed. $\square$

Declarations

Appendix

In this appendix, we always let Ω be a smooth and bounded domain in $\mathbb{R}^n$ ($n \ge 1$). Given $f \in C(\overline{\Omega})$, consider the following eigenvalue problem with Neumann boundary condition:

$$\begin{cases} -D\Delta\phi + f(x)\phi = \lambda\phi & \text{in } \Omega, \\ \frac{\partial\phi}{\partial\nu} = 0 & \text{on } \partial\Omega, \end{cases} \tag{A.1}$$

where $\nu(x)$ is the unit exterior normal vector of $\partial\Omega$ at x, and the coefficient D is a positive constant.

We start with a well-known fact concerning the asymptotic behavior of the principal eigenvalue of (A.1) with respect to small diffusion; one may refer to, for example, Lou and Nagylaki (2006, Lemma 3.1).

Lemma 5.1 *Let $\lambda_1(D, f)$ be the principal eigenvalue of (A.1). Then it holds that*

$$\lim_{D \to 0} \lambda_1(D, f) = \min_{x \in \overline{\Omega}} f(x).$$

We next recall the L^1-estimate for the weak solution [due to Brezis and Strauss (1973)] of the following linear elliptic problem:

$$-\Delta w + c(x)w = g \quad \text{in } \Omega, \qquad \frac{\partial w}{\partial \nu} = 0 \text{ on } \partial\Omega. \tag{A.2}$$

Lemma 5.2 (a) (Global estimates) *Assume that $c \in L^\infty(\Omega)$ and $g \in L^1(\Omega)$, and let $w \in W^{1,1}(\Omega)$ be a weak solution of (A.2). Then, for any $r \in [1, n/(n-1))$, we have $w \in W^{1,r}(\Omega)$ and the following estimate*

$$\|w\|_{W^{1,r}(\Omega)} \leq C(\|g\|_{L^1(\Omega)} + \|w\|_{L^1(\Omega)}),$$

where the positive constant C is independent of w.

(b) (Interior estimates) *Assume that $\Omega' \subset\subset \Omega$ is a smooth domain, $c \in L^\infty(\Omega)$, $g \in L^1(\Omega)$, and let $w \in W^{1,1}(\Omega)$ be a weak solution to the equation $-\Delta w + c(x)w = g$. Then, for any $r \in [1, n/(n-1))$, we have $w \in W^{1,r}(\Omega')$ and the following estimate*

$$\|w\|_{W^{1,r}(\Omega')} \leq C(\|g\|_{L^1(\Omega)} + \|w\|_{L^1(\Omega)}),$$

where the positive constant C is independent of w.

At last, we state a Harnack-type inequality for weak solutions [see, e.g., Lieberman (2005) or Peng et al. (2008)], whose strong form was obtained in Lin et al. (1988).

Lemma 5.3 (a) (Global Harnack inequality) *Let $c \in L^r(\Omega)$ for some $r > n/2$. If $w \in W^{1,2}(\Omega)$ is a non-negative weak solution of the boundary value problem*

$$-\Delta w + c(x)w = 0 \quad \text{in } \Omega, \qquad \frac{\partial w}{\partial \nu} = 0 \text{ on } \partial\Omega,$$

then there is a constant C, determined only by $\|c\|_r$, r and Ω such that

$$\sup_{\Omega} w \leq C \inf_{\Omega} w.$$

(b) (Local Harnack inequality) *Let $\Omega' \subset\subset \Omega$ be a smooth domain and $c \in L^r(\Omega)$ for some $r > n/2$. If $w \in W^{1,2}(\Omega)$ is a non-negative weak solution of the equation*

$-\Delta w + c(x)w = 0$, then there is a constant C, determined only by $\|c\|_r$, r, Ω and Ω', such that

$$\sup_{\Omega'} w \leq C \inf_{\Omega'} w.$$

References

Allen LJS, Bolker BM, Lou Y, Nevai AL (2007) Asymptotic profiles of the steady states for an SIS epidemic patch model. SIAM J Appl Math 67:1283–1309

Allen LJS, Bolker BM, Lou Y, Nevai AL (2008) Asymptotic profiles of the steady states for an SIS epidemic reaction–diffusion model. Discrete Contin Dyn Syst 21:1–20

Allen LJS, Bolker BM, Lou Y, Nevai AL (2009) Spatial patterns in a discrete-time SIS patch model. J Math Biol 58:339–375

Anderson RM, May RM (1979) Population biology of infectious diseases. Nature 280:361–367

Balcan D et al (2009) Multiscale mobility networks and the spatial spreading of infectious diseases. Proc Natl Acad Sci USA 106:21484–21489

Brezis H, Strauss WA (1973) Semi-linear second-order elliptic equations in L^1. J Math Soc Jpn 25:565–590

Britton T, Ball F, Trapman P (2020a) A mathematical model reveals the influence of population heterogeneity on herd immunity to SARS-CoV-2. Science 369:846–849

Britton T, Ball, F, Trapman P (2020b) The disease-induced herd immunity level for Covid-19 is substantially lower than the classical herd immunity level, preprint, arXiv:2005.03085

Brockmann D, Helbing D (2013) The hidden geometry of complex, network-driven contagion phenomena. Science 342:1337–1342

Castellano K, Salako RB (2022) On the effect of lowering population's movement to control the spread of an infectious disease. J Differ Equ 316:1–27

Cui R (2021) Asymptotic profiles of the endemic equilibrium of a reaction–diffusion–advection SIS epidemic model with saturated incidence rate. Discrete Contin Dyn Syst Ser B 26:2997–3022

Cui R, Lam K-Y, Lou Y (2017) Dynamics and asymptotic profiles of steady states of an epidemic model in advective environments. J Differ Equ 263:2343–2373

Cui R, Li H, Peng R, Zhou M (2021) Concentration behavior of endemic equilibrium for a reaction–diffusion–advection SIS epidemic model with mass action infection mechanism. Calc Var Partial Differ Equ, 60, paper no. 184, 38 pp

Cui R, Lou Y (2016) A spatial SIS model in advective heterogeneous environments. J Differ Equ 261:3305–3343

Deng K, Wu Y (2016) Dynamics of an SIS epidemic reaction–diffusion model. Proc R Soc Edinb Sect A 146:929–946

Di Lauro F, et al (2021) The impact of network properties and mixing on control measures and disease-induced herd immunity in epidemic models: a mean-field model perspective, preprint, arXiv:2007.06975

Du Z, Peng R (2016) A priori L^∞-estimate for solutions of a class of reaction–diffusion systems. J Math Biol 72:429–1439

Gao D (2019) Travel frequency and infectious diseases. SIAM J Appl Math 79:1581–1606

Gao D, Dong C-P (2020) Fast diffusion inhibits disease outbreaks. Proc Am Math Soc 148:1709–1722

Gao D, Ruan S (2011) An SIS patch model with variable transmission coefficients. Math Biosci 232:110–115

Ge J, Kim K, Lin Z, Zhu H (2015) A SIS reaction–diffusion–advection model in a low-risk and high-risk domain. J Differ Equ 259:5486–5509

Han S, Lei C (2019) Global stability of equilibria of a diffusive SEIR epidemic model with nonlinear incidence. Appl Math Lett 98:114–120

Hethcote HW (2000) The mathematics of infectious diseases. SIAM Rev 42:599–653

Jia JS et al (2020) Population flow drives spatio-temporal distribution of COVID-19 in China. Nature 582:389–394

Kermack WO, McKendrick AG (1927) Contributions to the mathematical theory of epidemics-I. Proc R Soc Lond Ser A 115:700–721

Kermack WO, McKendrick AG (1991) Contributions to the mathematical theory of epidemics-I. Bull Math Biol 53:33–55

Kermack WO, McKendrick AG (1991) Contributions to the mathematical theory of epidemics-II. The problem of endemicity. Bull Math Biol 53:57–87

Kermack WO, McKendrick AG (1991) Contributions to the mathematical theory of epidemics-III. Further studies of the problem of endemicity. Bull Math Biol 53:89–118

Kraemer MUG et al (2020) The effect of human mobility and control measures on the COVID-19 epidemic in China. Science 368:493–497

Kuto K, Matsuzawa H, Peng R (2017) Concentration profile of the endemic equilibria of a reaction–diffusion–advection SIS epidemic model. Calc Var Partial Differ Equ, 56, paper no. 112, 28 pp

Lei C, Li F, Liu J (2018) Theoretical analysis on a diffusive SIR epidemic model with nonlinear incidence in a heterogeneous environment. Discrete Contin Dyn Syst Ser B 23:4499–4517

Lei C, Xiong J, Zhou X (2020) Qualitative analysis on an SIS epidemic reaction–diffusion model with mass action infection mechanism and spontaneous infection in a heterogeneous environment. Discrete Contin Dyn Syst Ser B 25:81–98

Lei C, Zhou X (2022) Concentration phenomenon of the endemic equilibrium of a reaction–diffusion–advection SIS epidemic model with spontaneous infection. Discrete Contin Dyn Syst Ser B 27:3077–3100

Li B, Bie Q (2019) Long-time dynamics of an SIRS reaction–diffusion epidemic model. J Math Anal Appl 475:1910–1926

Li B, Li H, Tong Y (2017) Analysis on a diffusive SIS epidemic model with logistic source. Z Angew Math Phys, 68(4), Art. 96, 25

Li B, Zhou J, Zhou X (2020) Asymptotic profiles of endemic equilibrium of a diffusive SIS epidemic system with nonlinear incidence function in a heterogeneous environment. Proc Am Math Soc 148:4445–4453

Li H, Peng R (2019) Dynamics and asymptotic profiles of endemic equilibrium for SIS epidemic patch models. J Math Biol 79:1279–1317

Li H, Peng R, Wang F-B (2017) Vary total population enhances disease persistence: qualitative analysis on a diffusive SIS epidemic model. J Differ Equ 262:885–913

Li H, Peng R, Wang Z-A (2018) On a diffusive susceptible-infected-susceptible epidemic model with mass action mechanism and birth-death effect: analysis, simulations, and comparison with other mechanisms. SIAM J Appl Math 78:2129–2153

Li H, Peng R, Xiang T (2018) Dynamics and asymptotic profiles of endemic equilibrium for two frequency-dependent SIS epidemic models with cross-diffusion. Eur J Appl Math 31:26–56

Li MY, Shuai Z (2009) Global stability of an epidemic model in a patchy environment. Can Appl Math Q 17:175–187

Lieberman GM (2005) Bounds for the steady-state Sel'kov model for arbitrary p in any number of dimensions. SIAM J Math Anal 36:1400–1406

Lin CS, Ni WM, Takagi I (1988) Large amplitude stationary solutions to a chemotaxis system. J Differ Equ 72:1–27

Lou Y, Nagylaki T (2006) Evolution of a semilinear parabolic system for migration and selection without dominance. J Differ Equ 225:624–665

Magal P, Webb G, Wu Y (2018) On a vector-host epidemic model with spatial structure. Nonlinearity 31:5589–5614

Magal P, Webb G, Wu Y (2019) On the basic reproduction number of reaction–diffusion epidemic models. SIAM J Appl Math 79:284–304

Peng R (2009) Asymptotic profiles of the positive steady state for an SIS epidemic reaction–diffusion model. Part I. J Differ Equ 247:1096–1119

Peng R, Liu S (2009) Global stability of the steady states of an SIS epidemic reaction–diffusion model. Nonlinear Anal 71:239–247

Peng R, Shi J, Wang M (2008) On stationary patterns of a reaction–diffusion model with autocatalysis and saturation law. Nonlinearity 21:1471–1488

Peng R, Wu Y (2021) Global L^∞-bounds and long-time behavior of a diffusive epidemic system in a heterogeneous environment. SIAM J Math Anal 53:2776–2810

Peng R, Yi F (2013) Asymptotic profile of the positive steady state for an SIS epidemic reaction–diffusion model: effects of epidemic risk and population movement. Phys. D. 259:8–25

Peng R, Zhao X-Q (2012) A reaction–diffusion SIS epidemic model in a time-periodic environment. Nonlinearity 25:1451–1471

Peng R, Zhao X-Q (2015) Effects of diffusion and advection on the principal eigenvalue of a periodic-parabolic problem with applications. Calc Var Partial Differ Equ 54:1611–1642

Song P, Lou Y, Xiao Y (2019) A spatial SEIRS reaction–diffusion model in heterogeneous environment. J Differ Equ 267:5084–5114

Suo J, Li B (2019) Analysis on a diffusive SIS epidemic system with linear source and frequency-dependent incidence function in a heterogeneous environment. Math Biosci Eng 17:418–441

Tian H et al (2020) An investigation of transmission control measures during the first 50 days of the COVID-19 epidemic in China. Science 368:638–642

Tong Y, Lei C (2018) An SIS epidemic reaction–diffusion model with spontaneous infection in a spatially heterogeneous environment. Nonlinear Anal Real World Appl 41:443–460

Vargas-De-Leon C, Korobeinikov A (2013) Global stability of a population dynamics model with inhibition and negative feedback. J Math Med Biol 30:65–72

Wang J, Wu X (2023) Dynamics and profiles of a diffusive Cholera model with bacterial hyperinfectivity and distinct dispersal rates. J Dyn Differ Equ 35:1205–1241

Wang J, Wang J (2021) Analysis of a reaction–diffusion Cholera model with distinct dispersal rates in the human population. J Dyn Differ Equ 33:549–575

Wen X, Ji J, Li B (2018) Asymptotic profiles of the endemic equilibrium to a diffusive SIS epidemic model with mass action infection mechanism. J Math Anal Appl 458:715–729

Wodarz D, Christensen JP, Thomsen AR (2002) The importance of lytic and nonlytic immune responses in viral infections. Trends Immunol 23:194–200

Wodarz D, Nowak MA (2000) Immune response and viral phenotype: do replication rate and cytopathogenicity influence virus load? J Theor Med 2:113–127

Wu Y, Zou X (2016) Asymptotic profiles of steady states for a diffusive SIS epidemic model with mass action infection mechanism. J Differ Equ 261:4424–4447

Zhang J, Cui R (2020) Asymptotic behavior of an SIS reaction–diffusion–advection model with saturation and spontaneous infection mechanism. Z Angew Math Phys 71 paper no. 150, 21

Zhu S, Wang J (2020) Analysis of a diffusive SIS epidemic model with spontaneous infection and a linear source in spatially heterogeneous environment. Discrete Contin Dyn Syst Ser B 25:1999–2019

Zhu S, Wang J (2020) Asymptotic profiles of steady states for a diffusive SIS epidemic model with spontaneous infection and a logistic source. Commun Pure Appl Anal 19:3323–3340